NASA Technical Paper 1790

Temporal and Spatial Inconsistencies of Time-Split Finite-Difference Schemes

Douglas L. Dwoyer and Frank C. Thames

APRIL 1981

NASA

NASA Technical Paper 1790

Temporal and Spatial Inconsistencies of Time-Split Finite-Difference Schemes

Douglas L. Dwoyer and Frank C. Thames
Langley Research Center
Hampton, Virginia

National Aeronautics
and Space Administration

**Scientific and Technical
Information Branch**

1981

CONTENTS

SUMMARY

In a recently published work by Abarbanel and Gottlieb (NASA CR-159386), a new class of explicit time-split algorithms designed for application to the Navier-Stokes equations for compressible flow was developed. These algorithms, which utilize locally-one-dimensional (LOD) spatial steps, were shown to possess stability characteristics superior to those of other time-split schemes. In the present work, the properties of an implicit LOD method, analogous to the Abarbanel-Gottlieb algorithm, are examined using the two-dimensional heat conduction equation as the test problem. Both temporal and spatial inconsistencies inherent in the scheme are identified. The principal result of the present work is the development of a new consistent, implicit splitting approach. The relationship between this new method and other time-split implicit schemes is explained, and stability problems encountered with the method in three dimensions are discussed.

INTRODUCTION

Many of the methods currently in use for numerically solving the Navier-Stokes equations for compressible flow are based on the concept of time-split and fractional-step finite-difference schemes developed at length in reference 1. These schemes include the Douglas-Gunn type alternating-direction implicit (ADI) methods of Briley and McDonald (ref. 2) and Beam and Warming (ref. 3) and the time-split explicit approaches such as that of MacCormack and Baldwin (ref. 4). The primary impetus in the development of time-split schemes is to reduce the amount of computational work to advance the solution one time step. In an implicit method, direct inversion of the full matrix required to gain the solution of the algebraic system associated with the difference equations requires a prohibitive amount of computational effort. By (approximately) splitting the matrix, this computational effort can be substantially reduced. In explicit methods, the splitting of the equations so that the various operators are advanced separately allows one, in principle, to advance each of these steps at its own stability limit. Since the stability limit for some of the steps can be substantially larger than for others in a typical high Reynolds number flow, a savings in computational effort can be realized. Currently, available splitting schemes suffer from various shortcomings. The spatially split Douglas-Gunn type methods (e.g., refs. 2 and 3) have stability problems in three dimensions, while the time-split explicit method of reference 4 does not achieve the sought-after independence of stability criteria for the various split steps.

Recent work by Abarbanel and Gottlieb (ref. 5) has shed new light on the stability restriction of the time-split scheme of MacCormack and Baldwin (ref. 4) and opened up the possibility of a new class of implicit methods. In the current paper, the consistency of time-split schemes as introduced by Abarbanel and Gottlieb is examined, and a new consistent time-split finite-difference algorithm is introduced.

In the time-split scheme of reference 4, the mixed-derivative term for viscous flow in the Navier-Stokes equations is apportioned among the various space-split operators. Abarbanel and Gottlieb point out, through a stability analysis of the full (linearized) Navier-Stokes equations, that this does not constitute an optimal split in that the allowable time step for each split step is influenced by the mesh spacing associated with other split steps. In reference 5, Abarbanel and Gottlieb propose a new method of splitting in which the spatial operators of the Navier-Stokes equations are first split into hyperbolic (i.e., Euler equations), parabolic, and mixed-derivative operators, and then each of these operators is solved with a time-split explicit scheme. The method is thus akin to the locally-one-dimensional (LOD) schemes, i.e., schemes in which only one term in the spatial operator appears in each split step. This scheme is proven to be an optimally split scheme. Further work by Abarbanel and Gottlieb indicates that such an operator-split scheme, in which the LOD explicit-difference method is replaced by an LOD backward Euler implicit method (with the cross-derivative operator advanced explicitly), is unconditionally stable and possesses a very good smoothing rate (a desirable feature for the multigrid method). Such a method thus appears to offer an attractive alternative to the spatially split Douglas-Gunn schemes of references 2 and 3, which are known to have stability problems in three dimensions (ref. 6).

As a summary of the status of current finite-difference methods for solution of the three-dimensional Navier-Stokes equations, the desirable properties of an "ideal" scheme are listed:

1. Unconditional stability

2. Consistency

3. Temporal accuracy

4. Ability to recover steady-state solutions, when they exist, independently of the iteration history

5. Ability to perform required matrix inversions at a minimum of computational time

The currently used Douglas-Gunn methods of references 2 and 3 meet criteria 2 through 5. On the other hand, the implicit version of the scheme developed by Abarbanel and Gottlieb in reference 5 has been demonstrated to meet criterion 1, but its properties in regard to criteria 2 through 4 are unknown.

The motivation of the current investigation was to understand better the properties of the LOD-type algorithm as proposed in reference 5. The test problem studied was the solution of the heat conduction equation on the unit square subject to steady Dirichlet data. Numerical solutions to this problem using both explicit and implicit LOD schemes revealed two immediate difficulties: (1) a temporal inconsistency in the steady-state solution due to the operator splitting and (2) errors in the solution due to the application of boundary data. The first difficulty is well known and there are a variety of ways of alleviating it. The second difficulty is not so well known and is somewhat more subtle but has been studied to some extent in the Russian literature (ref. 1) and

is discussed briefly by Mitchell (ref. 7). The errors produced by the temporal inconsistency are of the order of the temporal truncation error and, hence, provide negligible contamination of the solution with explicit schemes, since stability considerations dictate that this time step be bounded below the spatial truncation error. However, stability requires no time-step bound for implicit schemes, so that the temporal inconsistency can actually swamp the true solution for large values of the time step. Computational verification of these errors for both explicit and implicit LOD schemes is presented in this paper.

As discussed in references 1, 7, and 8, the boundary-condition errors in the LOD methods arise from the fact that the intermediate solutions do not represent consistent approximations to the dependent variables at any time level. Hence, the intermediate boundary data may not properly be the given boundary data for the problem and, in general, will be dependent on the form of the split operator and the given boundary data. Consistently split schemes do not suffer from this problem, since all intermediate solutions represent approximations to the dependent variables at the new time level (ref. 8). The method of undetermined functions (MUD) developed in reference 1 is shown to alleviate the boundary difficulty for the LOD schemes for Dirichlet data. A generalization of this procedure leads to the construction of a general consistent LOD scheme which requires no boundary-error correction for steady data. This new approach is presented in the current work.

In the remainder of this paper the inconsistencies associated with LOD schemes are developed in detail and methods for their alleviation outlined. The information thus developed is used to devise a general consistent LOD scheme. Comments are then made on the relation of this scheme to other ADI schemes.

SYMBOLS

A_ℓ full-step tridiagonal-difference operator defined in equation (13), $\ell = 1,2$

$\tilde{A}_\ell$ half-step tridiagonal-difference operator defined in equation (30), $\ell = 1,2$

$\hat{A}_\ell$ partial-step tridiagonal-difference operator defined in equation (62), $\ell = 1,2$

B_ℓ full-step explicit-difference operator defined in equation (14), $\ell = 1,2$

d_ℓ boundary-condition residual function for LOD forward Euler scheme defined in equations (A3), $\ell = 1,\ldots 4$

D discrete computational domain (fig. 1)

D_c continuum domain (fig. 1)

D_1, D_2	union of all horizontal and vertical grid lines in D, respectively (fig. 1)
$\bar{D}_1, \bar{D}_2$	union of all horizontal and vertical grid lines in $D \cup \Gamma$, respectively (fig. 1)
e_ℓ	boundary-condition residual function for LOD Lax-Wendroff scheme defined in equations (A7), $\ell = 1,...4$
E	error in solution defined as difference between analytical and numerical solution
f_ℓ	boundary-condition function, $\ell = 1,...4$
F_ℓ	constants in exact solution to test problem, $\ell = 1,2$
g_ℓ	boundary-condition residual function for LOD backward Euler scheme defined in equations (33) to (36), $\ell = 1,...4$
$\tilde{g}_\ell$	boundary-condition residual function for LOD predictor-corrector scheme, $\ell = 1,...4$
$\hat{g}_\ell$	boundary-condition residual function for LODQ scheme defined in equations (69), $\ell = 1,...4$
G	Von Neumann damping ratio
h	spatial step size (subscripts indicate spatial direction)
H_j	horizontal grid line in D, $j = 1,2,...J$
i	$= \sqrt{-1}$
I	total number of spatial grid points in x_1-direction
J	total number of spatial grid points in x_2-direction
k	integer exponent
L_1, L_2, L_3	general time-split spatial-difference operators
M_1, M_2, M_3	general LOD split-difference operators
n	time-increment counter
q	correction function for LOD scheme determined by method of undetermined functions
Q	correction function for LODQ scheme
R	steady-state residual defined in equation (17)

$\tilde{R}$	steady-state residual of whole step form of time-split schemes
$\hat{R}$	error function of steady-state residual of time-split schemes
t	time
u	dependent variable
V_i	vertical grid line in D, $i = 1,2,\ldots I$
x_1, x_2, x_3	Cartesian coordinate directions
α	parameter that sets temporal order of accuracy
β_ℓ	$= 2\,\Delta t\, h^{-2}(1 - \cos\theta_\ell)$, $\ell = 1,2$
γ_ℓ	element of discrete boundary Γ, $\ell = 1,\ldots 4$
$\gamma_{c\ell}$	element of continuum boundary Γ_c, $\ell = 1,\ldots 4$
Γ	discrete boundary (fig. 1)
Γ_c	continuum boundary (fig. 1)
$\delta u/\delta t$	general time-difference approximation
$\delta u/\delta x_\ell$	spatial-difference approximation, $\ell = 1,2,3$
Δt	time step
η_ℓ	$= \Delta t\, h^{-1} \sin\theta_\ell$, $\ell = 1,2$
θ_ℓ	phase angle of Fourier error analysis, $\ell = 1,2$
Λ_ℓ	second-order central second-difference operator defined in equations (6) and (7), $\ell = 1,2$
τ	normalized time step defined in equation (20)
ω_ℓ	element of the set Ω, $\ell = 1,\ldots 4$
Ω	set of grid lines one mesh increment interior to discrete boundary Γ (fig. 1)

Superscripts:

n	time-step counter
m	time-step counter

(m) time-split-step counter

* intermediate time-level indicator

Subscripts:

i x_1-mesh increment counter

j x_2-mesh increment counter

max maximum

min minimum

1,2 Cartesian coordinate direction indicator

Abbreviations:

ADI alternating direction implicit

DG Douglas-Gunn

LOD locally-one-dimensional

LODBE LOD backward Euler

LODBEC consistent LOD backward Euler

LODFE LOD forward Euler

LODPC LOD predictor-corrector

LODQ LOD with correction function Q (eqs. (60) to (66))

MUD method of undetermined functions

MUDB MUD with boundary data adjusted

MUDF MUD with correction function applied over entire domain D

2-D two-dimensional

3-D three-dimensional

DEVELOPMENT AND APPLICATION OF SIMPLE LOD SCHEMES

MODEL PROBLEM FORMULATION

The model problem chosen for study in this paper is the heat conduction equation in two dimensions on the unit square. That is,

$$\frac{\partial u}{\partial t} = \frac{\partial^2 u}{\partial x_1^2} + \frac{\partial^2 u}{\partial x_2^2} \tag{1}$$

will be solved on the domain D_c, which is the open set

$$D_c \equiv \left\{(x_1, x_2) \; : \; 0 < x_1, x_2 < 1\right\}$$

The boundary of the continuum domain Γ_c is the union of the four unit-length line segments $\gamma_{c\ell}$, as illustrated in figure 1. The discrete domain D on which the computations are carried out is obtained by overlaying D_c with a uniform net, with D defined by

$$D \equiv \left\{\left[(x_1)_{ij}, (x_2)_{ij}\right] \; : \; (x_1)_{ij} = (i-1)h_1, (x_2)_{ij} = (j-1)h_2 \right.$$
$$\left. \text{for} \quad 2 \leqq i \leqq I-1, \; 2 \leqq j \leqq J-1 \right\}$$

where I and J are the number of mesh points in the x_1- and x_2-directions, respectively, and the mesh spacings are given by

$$h_1 \equiv \frac{1}{I-1} \qquad h_2 \equiv \frac{1}{J-1}$$

In all numerical solutions performed in this paper we will take $I = J$. Consequently, the spatial step sizes are equal (i.e., $h_1 = h_2$), so that the unsubscripted symbol h is used to denote both spatial increments. The discrete boundary of D, the set Γ, is the union of the four discrete line segment sets γ_ℓ, which have obvious definitions. The discrete region is depicted in figure 1. To augment the results which follow, the discrete set Ω is defined as the union of the four line segments ω_ℓ lying one mesh width from Γ within D (fig. 1).

As a final point, additional notation is introduced to simplify the description of the manner in which the algorithms described in this paper are performed computationally. Let

$$H_\ell \equiv \left\{\left[(x_1)_{ij}, (x_2)_{ij}\right] \; : \; 2 \leqq i \leqq I-1, \; j = \ell\right\}$$

$$V_\ell \equiv \left\{\left[(x_1)_{ij}, (x_2)_{ij}\right] \; : \; i = \ell, \; 2 \leqq j \leqq J-1\right\}$$

These two sets are illustrated in figure 1. Note that H_ℓ is the ℓth horizontal line and V_ℓ is the ℓth vertical line in $D \cup \Gamma$. Now, define

$$D_1 \equiv \bigcup_{\ell=2}^{J-1} H_\ell$$

$$\bar{D}_1 \equiv \bigcup_{\ell=1}^{J} H_\ell$$

$$D_2 \equiv \bigcup_{\ell=2}^{I-1} V_\ell$$

$$\bar{D}_2 \equiv \bigcup_{\ell=1}^{I} V_\ell$$

The sets D_1 and D_2 are equivalent to D but merely viewed in another way - as the union of all horizontal and vertical lines in D, respectively. The sets $\bar{D}_1$ and $\bar{D}_2$ include the adjacent boundary lines.

During the course of this paper, the numerical solution to equation (1) using various algorithms is discussed for two separate problems, designated test problem 1 and test problem 2 (or TP1 and TP2). Both problems have Dirichlet-type boundary data. Let

$$u(x_1,x_2,t) = f_\ell(x_1,x_2,t) \qquad (x_1,x_2) \in \gamma_{c\ell},\ \ell = 1,\ldots 4 \tag{2}$$

The boundary data for the test problems are

$$\left.\begin{aligned} f_1(x_1,x_2,t) &= F_1 \sin \pi x_2 \\ f_2(x_1,x_2,t) &= F_2 \sin \pi x_1 \\ f_3(x_1,x_2,t) &= F_1 \sin \pi x_2 \\ f_4(x_1,x_2,t) &= F_2 \sin \pi x_1 \end{aligned}\right\} \tag{3}$$

where F_1 and F_2 may take on the values 0 or 1. The steady-state analytic solution to equation (1) on D_c subject to the boundary data given by equations (3) is

$$u(x_1,x_2) = F_2 \operatorname{sech}\left(\frac{\pi}{2}\right) \cosh\left[\pi\left(x_2 - \frac{1}{2}\right)\right] \sin \pi x_1 + F_1 \operatorname{sech}\left(\frac{\pi}{2}\right) \cosh\left[\pi\left(x_1 - \frac{1}{2}\right)\right] \sin \pi x_2 \tag{4}$$

For TP1, $F_1 = 0$ and $F_2 = 1$; for TP2, $F_1 = 1$ and $F_2 = 0$. The boundary conditions and applicable steady-state analytic solutions for TP1 and TP2 are plotted for illustrative purposes in figure 2.

The reason for the introduction of the two separate test problems arises from the nature of the errors in time-split difference methods illustrated in this report. As discussed herein, errors are introduced in time-split methods as a result of inconsistencies associated with the boundary conditions. The particular boundaries associated with these errors vary depending on the particular time-split scheme, hence the need for the two problems.

DIFFERENCE APPROXIMATIONS

All numerical schemes discussed in this paper use first-order, one-sided (backward or forward) finite differences for the time derivatives and second-order, central differences for spatial derivatives appearing in equation (1). If u_{ij}^n is the approximation to $u(ih_1, jh_2, n\,\Delta t)$, then the difference forms are

$$\left(\frac{\partial u}{\partial t}\right)_{ij}^{n-p} \approx \frac{u_{ij}^n - u_{ij}^{n-1}}{\Delta t} \tag{5}$$

where $0 \leq p \leq 1$ and Δt is the time step. The spatial derivatives are approximated by

$$\left(\frac{\partial^2 u}{\partial x_1^2}\right)_{ij}^{n} \approx \frac{u_{i+1,j}^n - 2u_{ij}^n + u_{i-1,j}^n}{h_1^2} \tag{6a}$$

$$\equiv \Lambda_1 u_{ij}^n \tag{6b}$$

$$\left(\frac{\partial^2 u}{\partial x_2^2}\right)^n_{ij} \approx \frac{u^n_{i,j+1} - 2u^n_{ij} + u^n_{i,j-1}}{h_2^2} \tag{7a}$$

$$\equiv \Lambda_2 u^n_{ij} \tag{7b}$$

When no confusion can arise regarding a given spatial location, the notation given in equations (5) to (7) is simplified by dropping the subscripts on u. For example, the forward-time, centered-space approximation to equation (1) may be written as

$$\frac{u^n - u^{n-1}}{\Delta t} = (\Lambda_1 + \Lambda_2) u^{n-1} \tag{8}$$

with the implied understanding that this approximation is to be applied at all points in D.

TIME-SPLIT SCHEMES

General Idea

Time-split schemes are methods in which the computations associated with advancing a numerical approximation a time distance Δt are divided into a sequence of two or more substeps. This division is done to obtain an algorithm with less computational work than the whole-step scheme. Time-split methods may be implicit, explicit, or a combination - some implicit steps, some explicit steps. Combination-type schemes are often referred to as predictor-corrector or hybrid methods.

As an illustration of the splitting concept, consider a general two-step scheme for equation (1) which advances time from level n to $n + 1$. Such a scheme may be written in operational form as

$$\left(\frac{\delta u}{\delta t}\right)_1 = L_1(\Lambda_1 u, \Lambda_2 u) \tag{9a}$$

$$\left(\frac{\delta u}{\delta t}\right)_2 = L_2(\Lambda_1 u, \Lambda_2 u) \tag{9b}$$

where $\frac{\delta u}{\delta t}$ represents some approximation to $\frac{\partial u}{\partial t}$, and L_1 and L_2 are specified functions which define the nature of the splitting. The variable u with no time-level indicator is meant to imply that a number of time levels may be associated with each Λ_ℓ. Combining equations (9a) and (9b) gives the whole-step scheme, which is equivalent to the split scheme at interior mesh nodes (i.e., for points in D). The whole-step algorithms assume the general form

$$\frac{u^{n+1} - u^n}{\Delta t} = (\Lambda_1 + \Lambda_2)\left[(1 - \alpha)u^n + \alpha u^{n+1}\right] + \Delta t^k L_3(\Lambda_1 u, \Lambda_2 u) \tag{9c}$$

where k is an integer, and L_3 is an error term resulting from the split and depends explicitly on L_1 and L_2. Equation (9c) may not be valid on or near the boundary of D (e.g., on one of the lines in Ω). For locally-one-dimensional (LOD) splittings, each of the split operators (eqs. (9a) and (9b)) involves spatial derivatives in only one direction. Therefore, the general form of the time-split LOD schemes for equation (1) may be written as

$$\left(\frac{\delta u}{\delta t}\right)_1 = M_1(\Lambda_1 u) \tag{10a}$$

$$\left(\frac{\delta u}{\delta t}\right)_2 = M_2(\Lambda_2 u) \tag{10b}$$

with the corresponding whole step

$$\frac{u^{n+1} - u^n}{\Delta t} = (\Lambda_1 + \Lambda_2)\left[(1 - \alpha)u^n + \alpha u^{n+1}\right] + \Delta t^k M_3(\Lambda_1 u, \Lambda_2 u) \tag{10c}$$

The Douglas-Gunn Method

One of the most widely used implicit time-split methods is that due to Douglas and Gunn (ref. 9). For the scalar equation (1), the spatially split Douglas-Gunn (DG) scheme is

$$\frac{u^* - u^n}{\Delta t} = \Lambda_1 u^* + \Lambda_2 u^n \tag{11a}$$

$$\frac{u^{n+1} - u^n}{\Delta t} = \Lambda_1 u^* + \Lambda_2 u^{n+1} \tag{11b}$$

The asterisk is a symbol of convenience and can denote some intermediate time level, say $n\,\Delta t < t^* \leqq (n+1)\,\Delta t$. As shown in this section, however, for some time-split methods, u^* or other intermediate levels may not be a consistent approximation to the solution of equation (1). Note that for the DG scheme each split step (eqs. (11)) is a consistent approximation to equation (1).

From an operational standpoint, equations (11) may be rewritten as

$$A_1 u^* = B_2 u^n \qquad (x_1, x_2) \in D_1 \tag{12a}$$

$$A_2 u^{n+1} = u^n + \Delta t\, \Lambda_1 u^* \qquad (x_1, x_2) \in D_2 \tag{12b}$$

where

$$A_\ell = (1 - \Delta t\, \Lambda_\ell) \qquad \ell = 1, 2 \tag{13}$$

$$B_\ell = (1 + \Delta t\, \Lambda_\ell) \qquad \ell = 1, 2 \tag{14}$$

The equivalent whole-step DG algorithm is obtained as follows. Multiplying equation (12b) by A_1 yields

$$A_1 A_2 u^{n+1} = A_1 u^n + \Delta t\, \Lambda_1 (A_1 u^*) \tag{15a}$$

$$= A_1 u^n + \Delta t\, \Lambda_1 (B_2 u^n) \tag{15b}$$

Note we have commuted Λ_1 and A_1 to obtain equation (15a) and used equation (12a) to obtain equation (15b). If equation (15b) is expanded using the definitions given by equations (13) and (14), the equivalent DG whole-step formula in difference form is

$$\frac{u^{n+1} - u^n}{\Delta t} = (\Lambda_1 + \Lambda_2) u^{n+1} - \Delta t^2 \Lambda_1 \Lambda_2 \left(\frac{u^{n+1} - u^n}{\Delta t} \right) \qquad (x_1, x_2) \in D \tag{16}$$

The time-splitting error term for the DG method is formally second order in time and, in addition, is proportional to an approximation to the time derivative

u_t. If the problem being solved has a steady-state solution, the time-splitting error term would be expected to vanish as the steady solution is approached. However, this will not be true of an unsteady problem. The symbol R is used to denote the so-called steady-state residual:

$$R \equiv (\Lambda_1 + \Lambda_2)u \tag{17}$$

The entire residual for this and other schemes is denoted $\tilde{R}$. For the DG method, $\tilde{R}$ is given by

$$\tilde{R}^{n+1} \equiv (\Lambda_1 + \Lambda_2)u^{n+1} - \Delta t^2 \Lambda_1 \Lambda_2 \left(\frac{u^{n+1} - u^n}{\Delta t} \right) \tag{18}$$

The DG method is unconditionally stable, as may be verified by a simple Von Neumann analysis. The damping ratio G is given by

$$G = \frac{1 + \beta_1 \beta_2}{(1 + \beta_1)(1 + \beta_2)} \tag{19}$$

where $\beta_\ell = 2\ \Delta t\ h^{-2}(1 - \cos \theta_\ell)$.

The DG approach was applied to both TP1 and TP2. The method is implemented by first implicitly solving equation (12a) (via the Thomas algorithm) along all interior horizontal grid lines in D (i.e., D_1; see fig. 1). This is followed by a similar implicit solution of equation (12b) along all vertical lines in D (i.e., D_2). The time splitting thus has the computational effect of approximating the inversion of the original block tridiagonal matrix (from $(\Lambda_1 + \Lambda_2)u^{n+1}$) by a sequence of simpler scalar tridiagonal inversions of the unidirectional A_ℓ operators. The penalty for use of such an artifice is, of course, the time-splitting error. The computational results are summarized in table I for three different time steps. The normalized time step τ is defined by

$$\tau \equiv \frac{\Delta t}{\frac{1}{4} h^2} \tag{20}$$

where $\tau = 1$ corresponds to the stability limit of the unsplit forward-time, centered-space method of equation (8). Table I gives the maximum and minimum absolute errors $|E|_{max}$ and $|E|_{min}$ (the maximum steady-state residuals R were driven to machine zero, approximately 10^{-13}), which demonstrate the h^2-convergence of the computed solution to the exact solution. In these calculations the maximum errors occur at the center of the grid, as should be

expected since this location is farthest from the boundaries where the solution has no error.

Locally-One-Dimensional Methods

In this section three locally-one-dimensional methods are discussed: (1) the LOD forward Euler method, (2) the LOD backward Euler method, and (3) the LOD predictor-corrector method.

LOD forward Euler scheme.- The LOD forward Euler (LODFE) scheme is a two-step time-explicit approximation to equation (1). The two steps are

$$\frac{u^* - u^n}{\Delta t} = \Lambda_1 u^n \tag{21a}$$

$$\frac{u^{n+1} - u^*}{\Delta t} = \Lambda_2 u^* \tag{21b}$$

Using equation (14), the computational steps are

$$\left.\begin{aligned} u^* &= B_1 u^n && (x_1, x_2) \in D_1 \\ u^* &= f_\ell^* && (x_1, x_2) \in \gamma_\ell,\ \ell = 1,3 \end{aligned}\right\} \tag{22a}$$

$$\left.\begin{aligned} u^{n+1} &= B_2 u^* && (x_1, x_2) \in D_2 \\ u^{n+1} &= f_\ell^{n+1} && (x_1, x_2) \in \gamma_\ell,\ \ell = 2,4 \end{aligned}\right\} \tag{22b}$$

For TP1 and TP2 we take $f_\ell^* = f_\ell^{n+1} = f_\ell$ for $(x_1, x_2) \in \gamma_\ell$, $\ell = 1, \ldots 4$. It is easily verified that the stability restriction is $\tau \leq 2$. The equivalent whole-step method is obtained by substituting equations (22a) into equations (22b) and expanding the operators:

$$\frac{u^{n+1} - u^n}{\Delta t} = (\Lambda_1 + \Lambda_2)u^n + \Delta t\, \Lambda_1 \Lambda_2 u^n \qquad (x_1, x_2) \in D \tag{23}$$

Note that the time-splitting error term $\Delta t\, \Lambda_1 \Lambda_2 u^n$, unlike that for the DG scheme (eq. (16)), is first order in Δt and depends upon the function itself u^n rather than a form of u_t.

The solution, error, and residual maps generated by the LODFE algorithm applied to TP1 are presented in figure 3 for $\tau = 1$ and $\tau = 2$. Note that the maximum and minimum errors now depend upon Δt, as predicted by equation (23), and that the steady-state residual (eq. (17)) is no longer arbitrarily small as with the DG scheme. The error map in figure 3 introduces another interesting point - the maximum error and residual now appear along grid lines immediately adjacent to a boundary, that is, along elements of the set Ω. (See fig. 1.)

LOD backward Euler scheme.- The two-step implicit LOD backward Euler (LODBE) method for equation (1) is given by

$$\frac{u^* - u^n}{\Delta t} = \Lambda_1 u^* \tag{24a}$$

$$\frac{u^{n+1} - u^*}{\Delta t} = \Lambda_2 u^{n+1} \tag{24b}$$

with comparable computational steps

$$\left.\begin{aligned} A_1 u^* &= u^n && (x_1, x_2) \in D_1 \\ u^* &= f_\ell^* && (x_1, x_2) \in \gamma_\ell,\ \ell = 1,3 \end{aligned}\right\} \tag{25a}$$

$$\left.\begin{aligned} A_2 u^{n+1} &= u^* && (x_1, x_2) \in D_2 \\ u^{n+1} &= f_\ell^{n+1} && (x_1, x_2) \in \gamma_\ell,\ \ell = 2,4 \end{aligned}\right\} \tag{25b}$$

For TP1 and TP2 we take $f_\ell^* = f_\ell^{n+1} = f_\ell$ for $(x_1, x_2) \in \gamma_\ell$, $\ell = 1, \ldots 4$ and A_ℓ is defined in equation (13). Multiplying equations (25b) by A_1, substituting from equations (25a), and expanding, we obtain the equivalent LODBE whole-step equation

$$\frac{u^{n+1} - u^n}{\Delta t} = (\Lambda_1 + \Lambda_2) u^{n+1} - \Delta t\, \Lambda_1 \Lambda_2 u^{n+1} \qquad (x_1, x_2) \in D \tag{26}$$

Equation (26) indicates that the LODBE algorithm has a time-splitting error behavior similar to the LODFE scheme, namely, first-order temporal accuracy and a function-dependent splitting error. Computational results verify this,

as shown by the error, residual, and steady-state solution maps for $\tau = 1$, 10, and 1000 presented in figure 4. Again, the steady-state solution is highly dependent upon τ and the maximum error appears on the set Ω adjacent to the boundaries. Note, however, that the implicit nature of the LODBE scheme has led to a desirable property: the method is unconditionally stable.

LOD predictor-corrector scheme. Before proceeding to a detailed analysis of the errors that appear in LOD methods, we introduce one additional LOD algorithm, which Yanenko (ref. 1) calls the predictor-corrector splitting scheme and which we term LODPC. This approach combines a LODBE predictor with an explicit, leapfrog corrector in three steps as follows:

$$\frac{u^* - u^n}{\Delta t/2} = \Lambda_1 u^* \tag{27a}$$

$$\frac{u^{n+1/2} - u^*}{\Delta t/2} = \Lambda_2 u^{n+1/2} \tag{27b}$$

$$\frac{u^{n+1} - u^n}{\Delta t} = (\Lambda_1 + \Lambda_2) u^{n+1/2} \tag{27c}$$

The corresponding computational equations and whole-step scheme are

$$\left.\begin{aligned} \tilde{A}_1 u^* &= u^n && (x_1, x_2) \in D_1 \\ u^* &= f_\ell^* && (x_1, x_2) \in \gamma_\ell,\ \ell = 1,3 \end{aligned}\right\} \tag{28a}$$

$$\left.\begin{aligned} \tilde{A}_2 u^{n+1/2} &= u^* && (x_1, x_2) \in D_2 \\ u^{n+1/2} &= f_\ell^{n+1/2} && (x_1, x_2) \in \gamma_\ell,\ \ell = 2,4 \end{aligned}\right\} \tag{28b}$$

$$\left.\begin{aligned} u^{n+1} &= u^n + \Delta t\ (\Lambda_1 + \Lambda_2) u^{n+1/2} && (x_1, x_2) \in D \\ u^{n+1/2} &= f_\ell^{n+1} && (x_1, x_2) \in \gamma_\ell,\ \ell = 1, \ldots 4 \end{aligned}\right\} \tag{28c}$$

$$\frac{u^{n+1} - u^n}{\Delta t} = (\Lambda_1 + \Lambda_2)\left(\frac{u^{n+1} + u^n}{2}\right) - \frac{\Delta t^2}{4}\Lambda_1\Lambda_2\left(\frac{u^{n+1} - u^n}{\Delta t}\right) \qquad (x_1, x_2) \in D \qquad (29)$$

For TP1 and TP2 we take $f_\ell^* = f_\ell^{n+1/2} = f_\ell^{n+1} = f_\ell$ for $(x_1, x_2) \in \gamma_\ell$, $\ell = 1, \ldots 4$, and

$$\tilde{A}_\ell \equiv \left(1 - \frac{\Delta t}{2}\Lambda_\ell\right) \qquad (30)$$

The development of equation (29) requires the assumption of commutativity of the operator product $\tilde{A}_1\tilde{A}_2$ and $(\Lambda_1 + \Lambda_2)$. Note that the addition of the leap-frog corrector has had two effects on the whole-step formula as evidenced by equation (29). First, the method is now second order in time; second, the splitting error now is proportional to u_t rather than u. The LODPC method is also unconditionally stable. The discussion of LODPC computational results is presented in the section on complete consistent schemes.

SOURCES OF ERROR IN LOD SCHEMES

For the sake of completeness, the sources of error in the simple forward and backward Euler LOD schemes are discussed here. A major source of the error in these methods arises from the well-known fact that the whole-step formulas (i.e., the scheme with u^* eliminated) resulting from equations (21) and (24) are not consistent with equation (1). Another error arises from a lesser known source, that is, from errors due to the application of the boundary data. These two sources of error are termed temporal and spatial inconsistencies, respectively, in this report.

The spatial inconsistency for the backward Euler scheme (eqs. (24)) is discussed in detail here following Yanenko (ref. 1). Examination of the structure of this scheme reveals that calculations on the first sweep are influenced by boundary data applied along γ_1 and γ_3 but are in no way influenced by boundary data applied along γ_2 and γ_4. Similarly, on the second sweep the calculations are influenced by the boundary data applied along γ_2 and γ_4 and not influenced by the boundary data applied along γ_1 and γ_3. This fact is graphically demonstrated in figure 5. As shown, on a given sweep the effect of the spatial operator contained within the equation for the sweep renders the solution independent of data on any grid line except the one being swept. From equations (24), one also notes that as $\Delta t \to \infty$, the coupling between the two sweeps vanishes. One is thus left with the solution of two independent series of boundary-value problems on the two sweeps. This fact is further reflected in the damping of the scheme given by

$$G = \frac{1}{(1 + \beta_1)(1 + \beta_2)} \tag{31}$$

where G is the ratio of the amplitudes of the Fourier modes between successive time steps. From equation (31),

$$\lim_{\Delta t \to \infty} G = 0 \tag{32}$$

which indicates that one approaches a direct solution to some (incorrect) steady problem as the time step increases. This behavior is in contrast to that of the Douglas-Gunn scheme, in which the entire spatial operator appears in each sweep equation. (See eqs. (11).) Thus, calculations on each sweep are influenced by data applied on all four boundaries. For the Douglas-Gunn method, $G \to 1$ as $\Delta t \to \infty$.

The incompatibility of the two sweep equations (25) with the boundary data is illustrated by the fact that if equations (25a) is applied along the boundary segment γ_2, one has

$$f_2^* - f_2^n - \Delta t \, \Lambda_1 f_2^* = g_2 \qquad (x_1, x_2) \in \gamma_2 \tag{33a}$$

Now, if f_2 is a function of time and we try to identify f_2^* with some intermediate value of f, say $f_2^{n+1/2}$, then equation (33a) becomes

$$f_2^{n+1/2} - f_2^n - \Delta t \, \Lambda_1 f_2^{n+1/2} = g_2 \qquad (x_1, x_2) \in \gamma_2 \tag{33b}$$

Note that, in general, g_2 does not vanish. For steady boundary data, g_2 is

$$-\Delta t \, \Lambda_1 f_2 = g_2 \qquad (x_1, x_2) \in \gamma_2 \tag{33c}$$

which again does not vanish, in general. Also note that

$$g_2 \equiv 0 \qquad (x_1, x_2) \in D \cup \gamma_1 \cup \gamma_3 \cup \gamma_4 \tag{33d}$$

Similar relations along the other boundary segments may be written:

$$\left.\begin{aligned} f_4^* - f_4^n - \Delta t\, \Lambda_1 f_4^* &= g_4 \qquad (x_1, x_2) \in \gamma_4 \\ g_4 &\equiv 0 \qquad (x_1, x_2) \in D \cup \gamma_1 \cup \gamma_2 \cup \gamma_3 \end{aligned}\right\} \tag{34}$$

$$\left.\begin{aligned} f_1^{n+1} - f_1^* - \Delta t\, \Lambda_2 f_1^{n+1} &= g_1 \qquad (x_1, x_2) \in \gamma_1 \\ g_1 &\equiv 0 \qquad (x_1, x_2) \in D \cup \gamma_2 \cup \gamma_3 \cup \gamma_4 \end{aligned}\right\} \tag{35}$$

$$\left.\begin{aligned} f_3^{n+1} - f_3^* - \Delta t\, \Lambda_2 f_3^{n+1} &= g_3 \qquad (x_1, x_2) \in \gamma_3 \\ g_3 &\equiv 0 \qquad (x_1, x_2) \in D \cup \gamma_1 \cup \gamma_2 \cup \gamma_4 \end{aligned}\right\} \tag{36}$$

With these definitions, equations (25) are now rewritten as

$$\left.\begin{aligned} A_1 u^* &= u^n + (g_2 + g_4) \qquad (x_1, x_2) \in \bar{D}_1 \\ A_2 u^{n+1} &= u^* + (g_1 + g_3) \qquad (x_1, x_2) \in \bar{D}_2 \end{aligned}\right\} \tag{37}$$

If u^* is eliminated from equations (37), the whole-step scheme becomes

$$A_1 A_2 u^{n+1} = u^n + (g_2 + g_4) + A_1 (g_1 + g_3) \qquad (x_1, x_2) \in D \cup \Gamma$$

or, upon expanding,

$$\frac{u^{n+1} - u^n}{\Delta t} = (\Lambda_1 + \Lambda_2) u^{n+1} - \Delta t\, \Lambda_1 \Lambda_2 u^{n+1} + \Delta t^{-1} \left[(g_2 + g_4) + A_1 (g_1 + g_3) \right] \qquad (x_1, x_2) \in D \cup \Gamma \tag{38}$$

where $\Lambda_1 \Lambda_2 u^{n+1} \equiv 0$ for $(x_1, x_2) \in \Gamma$. Thus, the steady-state residual of the scheme given by equations (37) is

$$\tilde{R} = (\Lambda_1 + \Lambda_2)u - \Delta t\, \Lambda_1\Lambda_2 u$$
$$+ \Delta t^{-1}\left[(g_2 + g_4) + A_1 (g_1 + g_3)\right] \qquad (x_1, x_2) \in D \cup \Gamma \tag{39}$$

As noted in equations (33) to (36), the functions g_ℓ are nonzero only on the boundaries. However, as illustrated in figure 6, if $g_1 \neq 0$ on γ_1, then $A_1 g_1 \neq 0$ on ω_1 and similarly on ω_3. In fact,

$$A_1 g_1 = \begin{cases} -\dfrac{\Delta t}{h^2}\, g_1 & (x_1, x_2) \in \omega_1 \\ \\ 0 & \text{Elsewhere} \end{cases} \tag{40a}$$

$$A_1 g_3 = \begin{cases} -\dfrac{\Delta t}{h^2}\, g_3 & (x_1, x_2) \in \omega_3 \\ \\ 0 & \text{Elsewhere} \end{cases} \tag{40b}$$

Thus, we would expect that the incompatibility of the split sweep operators with boundary data applied in the sweep direction contributes an error term to the steady-state residual of the whole-step scheme only on Ω (eq. (39)). This incompatibility contributes an error term to the residual $\tilde{R}$ only on Ω because of the unique form of the functions g_ℓ; however, the error in the solution u caused by this term is propagated over the entire grid.

The errors present in the solutions in figure 4 are a result of the additional terms identified in the steady-state residual formula (eq. (39)); i.e.,

$$\hat{R} = -\Delta t\, \Lambda_1\Lambda_2 u + \Delta t^{-1} A_1 (g_1 + g_3) \qquad (x_1, x_2) \in D \tag{41}$$

as demonstrated in the next section. Note also from figure 4 that the maximum error occurs on Ω. This arises from the fact that the term $\Delta t^{-1} A_1 (g_1 + g_3)$ appearing in equation (41) is nonzero only on Ω.

Errors of the type discussed here are present in all time-split or LOD-type schemes. Similar boundary-error analyses are carried out for the LOD forward Euler, LOD Lax-Wendroff, and a hybrid LOD scheme in appendix A. Procedures designed to eliminate these errors from time-split schemes are introduced in the next section of this paper.

COMPLETE CONSISTENT LOD SCHEMES

REMOVAL OF TEMPORAL INCONSISTENCY

A desirable property of difference schemes for the solution of equation (1) is that they be accurate for the unsteady case and recover any existing steady-state solution independently of Δt. Such a scheme is designated "complete consistent" in reference 1. We now attempt to render the inconsistent LOD backward Euler method complete consistent through the removal of both the temporal and spatial inconsistencies. Removal of the temporal inconsistency is discussed first, since it is the most easily achieved. A similar modification of LODFE appears in appendix A.

The LODBE method can be made temporally consistent by the explicit addition of the term $\Delta t^2 \Lambda_1 \Lambda_2 u^n$ to the first step of the time-split operator. ($\Delta t^2 \Lambda_1 \Lambda_2 u^n$ is defined to be zero for $(x_1, x_2) \in \Gamma$.) Thus, the computational algorithm expressed by equations (37) becomes

$$A_1 u^* = u^n + \Delta t^2 \Lambda_1 \Lambda_2 u^n + (g_2 + g_4) \qquad (x_1, x_2) \in \bar{D}_1 \tag{42a}$$

$$A_2 u^{n+1} = u^* + (g_1 + g_3) \qquad (x_1, x_2) \in \bar{D}_2 \tag{42b}$$

where the boundary-condition residual functions have been retained for compatibility with analyses which follow later. In whole steps the scheme (eqs. (42)) is

$$\frac{u^{n+1} - u^n}{\Delta t} = (\Lambda_1 + \Lambda_2) u^{n+1} - \Delta t^2 \Lambda_1 \Lambda_2 \left(\frac{u^{n+1} - u^n}{\Delta t} \right)$$

$$+ \Delta t^{-1} \left[A_1 (g_1 + g_3) + (g_2 + g_4) \right] \qquad (x_1, x_2) \in D \cup \Gamma \tag{43}$$

Note the term that brings about the temporal inconsistency has been removed (for problems having a steady-state solution) by converting it to a u_t form. If we restrict our attention to D, g_2 and g_4 can be dropped from equation (43), since they are zero by definition on D, so that we obtain

$$\frac{u^{n+1} - u^n}{\Delta t} = (\Lambda_1 + \Lambda_2) u^{n+1} - \Delta t^2 \Lambda_1 \Lambda_2 \left(\frac{u^{n+1} - u^n}{\Delta t} \right)$$

$$+ \Delta t^{-1} \left[A_1 (g_1 + g_3) \right] \qquad (x_1, x_2) \in D \tag{44}$$

Recall that, in view of the analysis presented in the previous section, the term $A_1(g_1 + g_3)$ cannot be eliminated, as it is nonzero at certain locations in D. (See eqs. (40).) The method specified by equations (42) is termed the consistent LOD backward Euler method (LODBEC). The technique used here to remove the temporal inconsistency was suggested to the authors by David Gottlieb, of Tel Aviv University.

Another LOD scheme which is temporally consistent in its basic form - the LODPC method - was introduced earlier. If boundary-error problems are anticipated, the computational scheme given in equations (28) may be rewritten as

$$\tilde{A}_1 u^* = u^n + (\tilde{g}_2 + \tilde{g}_4) \qquad (x_1, x_2) \in \bar{D}_1 \tag{45a}$$

$$\tilde{A}_2 u^{n+1/2} = u^* + (\tilde{g}_1 + \tilde{g}_3) \qquad (x_1, x_2) \in \bar{D}_2 \tag{45b}$$

$$u^{n+1} = u^n + \Delta t(\Lambda_1 + \Lambda_2) u^{n+1/2} \qquad (x_1, x_2) \in D \tag{45c}$$

No new boundary residual terms have been introduced for the explicit corrector (eq. (45c)), since this step is consistent with equation (1). Formation of the whole-step scheme requires care, since the functions $\tilde{g}_\ell$ are discontinuous. Formulas derived for the contribution to the residual on D from the terms $\tilde{g}_\ell$ in which operator commutativity was assumed did not correctly predict the computed results. For this reason, no operator commutativity was assumed on g_ℓ in the following derivation. Therefore, formation of the scheme proceeds as follows. Multiplying equation (45b) by $\tilde{A}_1$ and substituting equation (45a) for $\tilde{A}_1 u^*$ yields

$$\tilde{A}_1 \tilde{A}_2 u^{n+1/2} = u^n + (\tilde{g}_2 + \tilde{g}_4) + \tilde{A}_1 (\tilde{g}_1 + \tilde{g}_3)$$

This equation may be solved by successively inverting the $\tilde{A}_1$ and $\tilde{A}_2$ operators:

$$u^{n+1/2} = \tilde{A}_2^{-1} \tilde{A}_1^{-1} u^n + \tilde{A}_2^{-1} \tilde{A}_1^{-1} \left[(\tilde{g}_2 + \tilde{g}_4) + \tilde{A}_1 (\tilde{g}_1 + \tilde{g}_3) \right]$$

Substituting this into equation (45c) for $u^{n+1/2}$ and multiplying the resulting equation by $\tilde{A}_1 \tilde{A}_2$ produces

$$\tilde{A}_1 \tilde{A}_2 u^{n+1} = \tilde{A}_1 \tilde{A}_2 u^n + \Delta t\, \tilde{A}_1 \tilde{A}_2 (\Lambda_1 + \Lambda_2) (\tilde{A}_1 \tilde{A}_2)^{-1} u^n$$

$$+ \Delta t\, \tilde{A}_1 \tilde{A}_2 (\Lambda_1 + \Lambda_2) \tilde{A}_2^{-1} \tilde{A}_1^{-1} \left[(\tilde{g}_2 + \tilde{g}_4) + \tilde{A}_1 (\tilde{g}_1 + \tilde{g}_3) \right]$$

Commuting the operators $\tilde{A}_1\tilde{A}_2$ and $(\Lambda_1 + \Lambda_2)$ that are operating only on u^n and simplifying the resulting equation gives the whole-step form:

$$\frac{u^{n+1} - u^n}{\Delta t} = (\Lambda_1 + \Lambda_2)\left(\frac{u^{n+1} + u^n}{2}\right) - \frac{\Delta t^2}{4}\Lambda_1\Lambda_2\left(\frac{u^{n+1} - u^n}{\Delta t}\right)$$

$$+ \tilde{A}_1\tilde{A}_2(\Lambda_1 + \Lambda_2)\tilde{A}_2^{-1}\tilde{A}_1^{-1}\left[(\tilde{g}_2 + \tilde{g}_4) + \tilde{A}_1(\tilde{g}_1 + \tilde{g}_3)\right] \qquad (x_1, x_2) \in D \qquad (46)$$

Figures 7 and 8 present the solutions obtained with LODBEC and LODPC, respectively. Note the minimum residual of machine zero and the large maximum residual on Ω. It is interesting that the residual is machine zero on grid points immediately adjacent to Ω for the LODBEC scheme for all time steps. (This is also true of the consistent LODFE scheme.) The boundary-error contribution to the residual moves in one extra row of grid points for the LODPC scheme, as shown in figure 8. This is apparently the effect of the complicated operator on $\tilde{g}$ in the last term of equation (46).

It is also interesting to compare the maximum residual from the computation with the predictions of equations (35) and (36) for the LODBEC scheme. For this scheme the steady-state residual is, from equation (44),

$$\tilde{R} = (\Lambda_1 + \Lambda_2)u + \frac{A_1(g_1 + g_3)}{\Delta t} \qquad (47)$$

where the term proportional to u_t has been dropped, since it vanishes as steady state is approached. Substitution of equations (3) into equations (35) and (36) and substitution of this result into equation (47) gives, for the residual,

$$\tilde{R} = (\Lambda_1 + \Lambda_2)u - \frac{\Delta t}{h^2}\Lambda_2 f_1 \qquad (x_1, x_2) \in \omega_1 \qquad (48)$$

$$\tilde{R} = R + \frac{\Delta t}{h^2}\pi^2 \sin \pi x_2 \qquad (x_1, x_2) \in \omega_1 \qquad (49)$$

Thus, if $R = 0$, i.e., if the scheme has converged to steady state, then

$$R = (\Lambda_1 + \Lambda_2)u = -\frac{\Delta t}{h^2}\pi^2 \sin \pi x_2 \qquad (50)$$

and, hence

$$|R|_{max} = \frac{\Delta t}{h^2}\pi^2 \tag{51}$$

The computed results are compared with results predicted by equation (51) in table II for various values of τ for a grid with $h = 1/8$. The computed and predicted results agree to within the spatial truncation error. The third column in table II gives the values predicted by equation (51) with $\Lambda_2 f_1$ evaluated discretely. The perfect agreement of the predicted and computed results confirms the validity of equations (33) to (36).

REMOVAL OF SPATIAL INCONSISTENCY

The first method for the removal of the spatial inconsistency investigated in the present work is the method of undetermined functions (MUD) as developed in reference 1. The method of undetermined functions can be cast in two forms: one in which the boundary data are adjusted (MUDB) and another in which a correction function is applied over the entire domain D (MUDF). Understanding of MUD is essential to understanding the development of the general consistent scheme given later.

Boundary-Point Method (MUDB)

The basis for the MUDB LODBEC scheme lies in the equations defining g_ℓ, i.e., equations (33) to (36), and the observation that since each of the steps in the method given by equations (42) is not consistent with equation (1), then u^* is not necessarily an approximation to u at any time level. We are thus free to view f^* as unknown boundary data which can be adjusted to yield a consistent whole-step scheme. In particular, if we set $g_1 = g_3 = 0$, then equations (35) and (36) an be solved for f_1^* and f_3^*:

$$f_1^* = f_1^{n+1} - \Delta t\, \Lambda_2 f_1^{n+1} = A_2 f_1^{n+1} \qquad (x_1, x_2) \in \gamma_1 \tag{52a}$$

$$f_3^* = f_3^{n+1} - \Delta t\, \Lambda_2 f_3^{n+1} = A_2 f_3^{n+1} \qquad (x_1, x_2) \in \gamma_3 \tag{52b}$$

These modified boundary data are now applied on the first sweep for the calculation of u^*. Similar formulas for the calculation of f^* for the consistent LOD forward Euler scheme (LODFEC) are presented in appendix A.

Field Correction Method (MUDF)

A more general method of undetermined functions (MUDF) may be used to correct for the boundary error in a way that allows use of the given boundary data in the calculations. For this method the LODBEC equations (eqs. (42)) are rewritten as

$$A_1 u^* = u^n + \Delta t^2 \Lambda_1 \Lambda_2 u^n \qquad (x_1, x_2) \in D_1 \tag{53a}$$

$$A_2 u^{n+1} = u^* + q \qquad (x_1, x_2) \in D_2 \tag{53b}$$

The unknown function q is introduced in equation (53b) for the purpose of absorbing the error in D due to the application of the given boundary data. The whole-step scheme becomes

$$\frac{u^{n+1} - u^n}{\Delta t} = (\Lambda_1 + \Lambda_2) u^{n+1} - \Delta t^2 \Lambda_1 \Lambda_2 \frac{\left(u^{n+1} - u^n\right)}{\Delta t} + A_1 q \qquad (x_1, x_2) \in D \tag{54}$$

Obviously in equation (54) we want $A_1 q = 0$ for $(x_1, x_2) \in D$. We set

$$\left.\begin{aligned} q &= g_1 \qquad (x_1, x_2) \in \gamma_1 \\ q &= g_3 \qquad (x_1, x_2) \in \gamma_3 \end{aligned}\right\} \tag{55}$$

The desired correction function q is obtained along each x_2 = Constant grid line (i.e., each H_j in D_1) by solving

$$A_1 q = 0 \qquad (x_1, x_2) \in D_1 \tag{56}$$

along each such line subject to the boundary conditions given by equations (55).

Results of computations using the LODBEC scheme with the spatial inconsistency corrected by MUDB and MUDF are presented in figure 9. (Results of both methods are identical.) Note on the figure 9 residual map the random distribution of machine zero residual over the entire grid and on the error map the maximum error at the middle of the grid. The results of these computations agree exactly with the results in table I. This agreement verifies that the scheme reproduces the exact solution to the difference equations generated with the Douglas-Gunn scheme for all three values of τ. We thus term this scheme, i.e., LODBEC with MUD, complete consistent.

A SELF-CANCELING BOUNDARY-ERROR SCHEME

Attempts to use a rigorous development of MUD for the LODPC scheme in the present investigation met with failure. The authors were able to develop a successful formulation of MUDF only by trial and error. It is thought that the reason for the failure to rigorously derive the proper field correction function was the requirement to assume operator commutativity in order to obtain analytic formulas. Rather than presenting a detailed discussion of this situation, we take here a more fruitful approach. Elimination of u* between equations (45a) and (45b) gives

$$u^n = \tilde{A}_1 \tilde{A}_2 u^{n+1/2} - \left(\tilde{g}_2^n + \tilde{g}_4^n\right) - \tilde{A}_1\left(\tilde{g}_1^n + \tilde{g}_3^n\right) \tag{57}$$

Similarly,

$$u^{n+1} = \tilde{A}_1 \tilde{A}_2 u^{n+3/2} - \left(\tilde{g}_2^{n+1} + \tilde{g}_4^{n+1}\right) - \tilde{A}_1\left(\tilde{g}_1^{n+1} + \tilde{g}_3^{n+1}\right) \tag{58}$$

Substitution of equations (57) and (58) into equation (45c) gives

$$\frac{u^{n+3/2} - u^{n+1/2}}{\Delta t} = (\Lambda_1 + \Lambda_2)\frac{\left(u^{n+3/2} + u^{n+1/2}\right)}{2} - \frac{\Delta t^2}{4}\Lambda_1\Lambda_2\frac{\left(u^{n+3/2} - u^{n+1/2}\right)}{\Delta t}$$

$$+ \left(\frac{\tilde{g}_2^{n+1} - \tilde{g}_2^n}{\Delta t}\right) + \left(\frac{\tilde{g}_4^{n+1} - \tilde{g}_4^n}{\Delta t}\right) + \tilde{A}_1\left[\left(\frac{\tilde{g}_1^{n+1} - \tilde{g}_1^n}{\Delta t}\right) + \left(\frac{\tilde{g}_3^{n+1} - \tilde{g}_3^n}{\Delta t}\right)\right] \tag{59}$$

Equation (59) indicates that the LODPC scheme is complete consistent for the (n+1/2) level data. In addition, note that no assumptions of operator commutativity were necessary to obtain equation (59). Computation with this method on the test problem produces results identical with results from the Douglas-Gunn method and from LODBEC with MUD. Note, however, that no modification of the boundary data had to be made to achieve these results. Also note that the n-level data converge to a different steady state than the (n+1/2) level data. (See fig. 8 for the n-level solution to the test problem.) Thus the n-level data may be viewed as data that have been preconditioned by including the negative of the values of both the temporal and spatial inconsistency errors. Thus, the LODPC scheme, with the (n+1/2) level data monitored as the solution, is a self-correcting LOD method which is complete consistent. To the authors' knowledge this result has not been observed before.

A GENERAL COMPLETE CONSISTENT LOD SCHEME

The field method of undetermined functions (MUDF) may be used to develop a class of complete consistent LOD schemes. We will develop the algorithm first in two dimensions, demonstrate the accuracy with computational results, and then extend the method to an arbitrary number of split steps.

We begin the development by writing the form of the desired whole-step formula

$$u^{n+1} = u^n + \Delta t(\Lambda_1 + \Lambda_2)\left[\alpha u^{n+1} + (1 - \alpha)u^n\right] - \alpha^2 \Delta t^3 \Lambda_1 \Lambda_2 \frac{\left(u^{n+1} - u^n\right)}{\Delta t} \qquad (60)$$

where $0 \leqq \alpha \leqq 1$. The LOD scheme is then

$$\hat{A}_1 u^* = Q^n + \left(\hat{g}_2^{n+1} + \hat{g}_4^{n+1}\right) \qquad (x_1, x_2) \in \bar{D}_1 \qquad (61a)$$

$$\hat{A}_2 u^{n+1} = u^* + \left(\hat{g}_1^{n+1} + \hat{g}_3^{n+1}\right) \qquad (x_1, x_2) \in \bar{D}_2 \qquad (61b)$$

where

$$\hat{A}_\ell = (1 - \alpha\, \Delta t\, \Lambda_\ell) \qquad \ell = 1, 2 \qquad (62)$$

and $\hat{g}_\ell$ with $\ell = 1, \ldots 4$ are error terms due to the application of boundary data and are analogous to the g_ℓ of LODBE. Here Q^n is introduced to absorb the temporal and spatial error. Elimination of u^* from equations (61) gives

$$u^{n+1} = Q^n + \alpha\, \Delta t(\Lambda_1 + \Lambda_2)u^{n+1} - \alpha^2 \Delta t^2 \Lambda_1 \Lambda_2 u^{n+1} + \left(\hat{g}_2^{n+1} + \hat{g}_4^{n+1}\right)$$

$$+ \hat{A}_1\left(\hat{g}_1^{n+1} + \hat{g}_3^{n+1}\right) \qquad (x_1, x_2) \in D \cup \Gamma \qquad (63)$$

Now equation (63) is subtracted from equation (60) and the result is solved for Q^n:

$$Q^n = u^n + (1 - \alpha)\, \Delta t(\Lambda_1 + \Lambda_2)u^n + \alpha^2 \Delta t^2 \Lambda_1 \Lambda_2 u^n$$

$$- \left(\hat{g}_2^{n+1} + \hat{g}_4^{n+1}\right) - \hat{A}_1\left(\hat{g}_1^{n+1} + \hat{g}_3^{n+1}\right) \qquad (x_1, x_2) \in D \cup \Gamma \qquad (64)$$

By making use of equation (63) rewritten for u^n, this result can be stated as

$$Q^n = Q^{n-1} + \Delta t(\Lambda_1 + \Lambda_2)u^n - \left(\hat{g}_2^{n+1} - \hat{g}_2^n\right) - \left(\hat{g}_4^{n+1} - \hat{g}_4^n\right)$$

$$- \hat{A}_1\left[\left(\hat{g}_1^{n+1} - \hat{g}_1^n\right) + \left(\hat{g}_3^{n+1} - \hat{g}_3^n\right)\right] \qquad (x_1, x_2) \in D \cup \Gamma \tag{65}$$

For steady boundary data, equation (65) reduces to

$$Q^n = Q^{n-1} + \Delta t(\Lambda_1 + \Lambda_2)u^n \qquad (x_1, x_2) \in D \tag{66}$$

The scheme developed above is termed the LODQ scheme. For steady boundary data, the heretofore unspecified $\hat{g}$ functions in equation (65) may be dropped without introducing any error. For unsteady boundary data, however, neglect of the $\hat{g}$ function terms appearing in equation (65) produces an $O(\Delta t)$ truncation error, as is now demonstrated. The terms due to $\hat{g}_2$ and $\hat{g}_4$ need not be considered, since they will not affect the solution on the interior of the domain. A derivation completely analogous to that yielding equations (40) gives for $\hat{g}_1$ and $\hat{g}_3$

$$\hat{A}_1\left(\hat{g}_1^{n+1} - \hat{g}_1^n\right) = \frac{-\alpha\ \Delta t}{h^2}\left(\hat{g}_1^{n+1} - \hat{g}_1^n\right) \qquad (x_1, x_2) \in \omega_1 \tag{67a}$$

$$\hat{A}_1\left(\hat{g}_3^{n+1} - \hat{g}_3^n\right) = \frac{-\alpha\ \Delta t}{h^2}\left(\hat{g}_3^{n+1} - \hat{g}_3^n\right) \qquad (x_1, x_2) \in \omega_3 \tag{67b}$$

Also, in the same way equations (35) and (36) were developed, expressions for $\hat{g}_1$ and $\hat{g}_3$ are obtained:

$$\hat{g}_1^{n+1} = f_1^{n+1} - f_1^* - \alpha\ \Delta t\ \Lambda_2 f_1^{n+1} \qquad (x_1, x_2) \in \gamma_1 \tag{68a}$$

$$\hat{g}_3^{n+1} = f_3^{n+1} - f_3^* - \alpha\ \Delta t\ \Lambda_2 f_3^{n+1} \qquad (x_1, x_2) \in \gamma_3 \tag{68b}$$

For convenience, we now take $f_1^* = f_1^{n+1}$ and $f_3^* = f_3^{n+1}$. Then equations (68) become

$$\hat{g}_1^{n+1} = -\alpha\ \Delta t\ \Lambda_2 f_1^{n+1} \qquad (x_1, x_2) \in \gamma_1 \tag{69a}$$

$$\hat{g}_3^{n+1} = -\alpha\ \Delta t\ \Lambda_2 f_3^{n+1} \qquad (x_1, x_2) \in \gamma_3 \tag{69b}$$

Substitution of equations (69) into equations (67) then gives

$$\hat{A}_1\left(\hat{g}_1^{n+1} - \hat{g}_1^{n}\right) = \frac{\alpha\ \Delta t}{h^2}\ \alpha\ \Delta t\ \Lambda_2\left(f_1^{n+1} - f_1^{n}\right) \qquad (x_1, x_2) \in \gamma_1 \tag{70a}$$

$$\hat{A}_1\left(\hat{g}_3^{n+1} - \hat{g}_3^{n}\right) = \frac{\alpha\ \Delta t}{h^2}\ \alpha\ \Delta t\ \Lambda_2\left(f_3^{n+1} - f_3^{n}\right) \qquad (x_1, x_2) \in \gamma_3 \tag{70b}$$

The reconstructed whole-step formula thus becomes, with the use of equation (66) for Q,

$$\frac{u^{n+1} - u^n}{\Delta t} = (\Lambda_1 + \Lambda_2)\left[\alpha u^{n+1} + (1 - \alpha)u^n\right] - \alpha^2\ \Delta t^2 \Lambda_1 \Lambda_2\ \frac{\left(u^{n+1} - u^n\right)}{\Delta t}$$

$$+ \alpha^2\left(\frac{\Delta t}{h^2}\right)\ \Delta t\ \Lambda_2\left[\left(\frac{f_1^{n+1} - f_1^{n}}{\Delta t}\right) + \left(\frac{f_3^{n+1} - f_3^{n}}{\Delta t}\right)\right] \qquad (x_1, x_2) \in D \tag{71}$$

Now proceeding to the limit of vanishing mesh according to the law $\Delta t/h^2 = \text{Constant}$ shows that the scheme is consistent with equation (1) to $O(\Delta t)$.

The complete consistent LODQ scheme may be summarized as

$$\hat{A}_1 u^* = Q^n \qquad (x_1, x_2) \in D_1 \tag{72a}$$

$$\hat{A}_2 u^{n+1} = u^* \qquad (x_1, x_2) \in D_2 \tag{72b}$$

$$Q^{n+1} = Q^n + \Delta t(\Lambda_1 + \Lambda_2)u^{n+1} \qquad (x_1, x_2) \in D \tag{72c}$$

where Q^0 may be taken as u^0. It should be borne in mind that for problems with unsteady boundary data, the scheme is first order in time regardless of the value of α. In order to achieve the possibility of second-order accuracy in time, i.e., to recover the whole-step formula given by equation (60) rather than that given by equation (71), one must evaluate the $\hat{g}$-functions. Further, it should be noted that operator commutativity does not have to be used to derive the equation for Q nor to develop the whole-step formula.

The scheme given in equations (72) was run on TP2 with the results summarized in figure 10. The numerical solutions agreed to machine accuracy for all values of α and Δt with the Douglas-Gunn scheme results.

The scheme can be readily extended to the case of m split steps as

$$\left.\begin{aligned} \hat{A}_1 u^{(1)} &= Q^n \\ \hat{A}_2 u^{(2)} &= u^{(1)} \\ &\cdot \quad\quad \cdot \\ &\cdot \quad\quad \cdot \\ &\cdot \quad\quad \cdot \\ \hat{A}_m u^{n+1} &= u^{(m-1)} \\ Q^{n+1} &= Q^n + \Delta t(\Lambda_1 + \Lambda_2 + \cdots + \Lambda_m) u^{n+1} \end{aligned}\right\} \qquad (73)$$

The scheme can be verified to be complete consistent by elimination of all intermediate values of $u^{(m)}$ and Q. (The whole-step scheme for the 3-D case is given in appendix A.) The scheme is also first order in time for unsteady data regardless of the value of α. Again, operator commutativity does not have to be assumed in order to derive these results.

A comment should be made about the stability of the LODQ scheme. As shown in appendix B, the method is unconditionally stable in two dimensions for both linear parabolic (heat conduction) and hyperbolic (advection) model equations for second-order central differences. In three dimensions, however, the method retains unconditional stability for the parabolic case only. In the three-dimensional hyperbolic case, the method is unconditionally unstable for second-order central differences. This unfortunate result follows from the desired whole-step formula, which contains the destabilizing term $\alpha^3 \Delta t^3 \delta^4 u / \delta x_1 \delta x_2 \delta x_3 \delta t$. One can eliminate this term from the whole-step formula, but to do so would generate a form of Q which would destroy the tridiagonal structure of one of the sweeps. This instability thus appears to be inherent in schemes for three dimensions which involve three spatially split implicit steps and two time levels, including the two-level Douglas-Gunn type schemes.

CONCLUDING REMARKS

It is obvious from the results presented in this paper that one must be very careful when applying locally-one-dimensional (LOD) type splitting schemes. Two types of errors present in such schemes have been explored in detail: the temporal inconsistency due to splitting and the spatial inconsistency due to application of Dirichlet boundary data. The temporal error has been shown to be of the order of the temporal truncation error of the scheme and, hence, does not have a large effect on the solution for explicit methods, in which one is forced to take small time steps from stability considerations. For implicit methods, however, the errors introduced by this inconsistency can be substantial when large time steps are taken. Care must therefore be taken to remove this inconsistency in implicit schemes.

The spatial inconsistency due to the application of Dirichlet data is somewhat more troubling. As has been shown, this inconsistency produces $O(1)$ truncation error terms on grid lines adjacent to the boundaries and, hence, can have a substantial effect on solution accuracy even at small time steps Δt. For the test problem examined in the present work, the errors in the solution caused by this inconsistency proved to be acceptable (i.e., $O(h^2)$, where h is spatial step size) at time steps of the order of the explicit stability limit, but such may not be the case for other problems.

As a result of these observations a complete consistent LOD scheme has been developed. For steady Dirichlet boundary data, the method eliminates both identified inconsistencies exactly; but, for unsteady Dirichlet data, the spatial inconsistency is made $O(\Delta t)$ rather than $O(1)$. This complete consistent scheme was developed in such a way as to produce a whole-step formula identical with that which is associated with the spatially split Douglas-Gunn method. As a consequence of this development the complete consistent locally-one-dimensional scheme (LODQ) can be considered an alternate interpretation of a general class of complete consistent ADI schemes which also includes the spatially split Douglas-Gunn method. All the strengths and weaknesses of this class of schemes are thus shared by the LODQ scheme.

One of the principal shortcomings of the whole-step formula associated with the LODQ scheme is its unconditional instability for the 3-D linear advection equation. With the introduction of the method for development of the LODQ scheme, one has substantial freedom, however, in the choice of resulting whole-step formula. It may be possible to devise a whole-step formula which can be spatially split, complete consistent, and second order in space and still be stable for the three-dimensional advection equation (e.g., by introduction of another time level). These possibilities were not examined in the current investigation.

One further comment should be made regarding the errors associated with LOD schemes. The time-split MacCormack-Baldwin method for the linear problem examined in this work reduces to the LOD Lax-Wendroff scheme given in appendix A. As shown in equations (A6) through (A7) this method contains the spatial inconsistency and, as demonstrated in equation (A8), also contains a temporal inconsistency. Computational experience of the authors verified these formulas.

The inclusion of the cross-derivative terms in each split step of the MacCormack-Baldwin method for the full Navier-Stokes equations may circumvent the spatial inconsistency encountered in the present work. On the basis of the present results, however, one would anticipate the spatial inconsistency to appear in the implementation of the optimal splitting developed in NASA CR-159386.

Langley Research Center
National Aeronautics and Space Administration
Hampton, VA 23665
February 13, 1981

APPENDIX A

OTHER LOD SCHEMES

CONSISTENT LOD FORWARD EULER SCHEME

In order to render the LOD forward Euler method complete consistent, a correction term similar to that in equation (42a) is introduced. Only the boundary method of undetermined functions (MUDB) for rendering the scheme complete consistent will be given. The algorithm is

$$u^* = B_1 u^n + \left(d_2^n + d_4^n\right) \qquad (x_1, x_2) \in D \cup \Gamma \tag{A1}$$

$$u^{n+1} = B_2 u^* - \Delta t^2 \Lambda_1 \Lambda_2 u^n + \left(d_1^n + d_3^n\right) \qquad (x_1, x_2) \in D \cup \Gamma \tag{A2}$$

where $\Lambda_1 \Lambda_2 u^n \equiv 0$ for $(x_1, x_2) \in \Gamma$, and

$$d_1^n = f_1^{n+1} - f_1^* - \Delta t\, \Lambda_2 f_1^* \qquad (x_1, x_2) \in \gamma_1 \tag{A3a}$$

$$d_2^n = f_2^* - f_2^n - \Delta t\, \Lambda_1 f_2^n \qquad (x_1, x_2) \in \gamma_2 \tag{A3b}$$

$$d_3^n = f_3^{n+1} - f_3^* - \Delta t\, \Lambda_2 f_3^* \qquad (x_1, x_2) \in \gamma_3 \tag{A3c}$$

$$d_4^n = f_4^* - f_4^n - \Delta t\, \Lambda_1 f_4^n \qquad (x_1, x_2) \in \gamma_4 \tag{A3d}$$

The whole-step formula is

$$\frac{u^{n+1} - u^n}{\Delta t} = (\Lambda_1 + \Lambda_2) u^n + \Delta t^{-1} B_2 \left(d_2^n + d_4^n\right) \qquad (x_1, x_2) \in D \tag{A4}$$

In order to render the scheme complete consistent, we set $d_2^n = d_4^n = 0$ by adjusting f_2^* and f_4^* according to the formulas

APPENDIX A

$$f_2^* = f_2^n + \Delta t\, \Lambda_1 f_2^n \qquad (x_1, x_2) \in \gamma_2 \tag{A5a}$$

$$f_4^* = f_4^n + \Delta t\, \Lambda_1 f_4^n \qquad (x_1, x_2) \in \gamma_4 \tag{A5b}$$

Computational experiments conducted by the authors demonstrated the complete consistency of the above outlined method.

LOD LAX-WENDROFF SCHEME

An LOD scheme based on the classic one-step Lax-Wendroff scheme can be written as

$$u^* = B_1 u^n + \frac{1}{2}\Delta t^2 \Lambda_1 \Lambda_1 u^n + \left(e_2^n + e_4^n\right) \qquad (x_1, x_2) \in \bar{D}_1 \tag{A6a}$$

$$u^{n+1} = B_2 u^* + \frac{1}{2}\Delta t^2 \Lambda_2 \Lambda_2 u^* + \left(e_1^n + e_3^n\right) \qquad (x_1, x_2) \in \bar{D}_2 \tag{A6b}$$

where

$$e_1^n = f_1^{n+1} - f_1^* - \Delta t\, \Lambda_2 f_1^* - \frac{1}{2}\Delta t^2 \Lambda_2 \Lambda_2 f_1^* \qquad (x_1, x_2) \in \gamma_1 \tag{A7a}$$

$$e_2^n = f_2^* - f_2^n - \Delta t\, \Lambda_1 f_2^n - \frac{1}{2}\Delta t^2 \Lambda_1 \Lambda_1 f_2^n \qquad (x_1, x_2) \in \gamma_2 \tag{A7b}$$

$$e_3^n = f_3^{n+1} - f_3^* - \Delta t\, \Lambda_2 f_3^* - \frac{1}{2}\Delta t^2 \Lambda_2 \Lambda_2 f_3^* \qquad (x_1, x_2) \in \gamma_3 \tag{A7c}$$

$$e_4^n = f_4^* - f_4^n - \Delta t\, \Lambda_1 f_4^n - \frac{1}{2}\Delta t^2 \Lambda_1 \Lambda_1 f_4^n \qquad (x_1, x_2) \in \gamma_4 \tag{A7d}$$

APPENDIX A

The whole-step scheme is

$$\frac{u^{n+1} - u^n}{\Delta t} = (\Lambda_1 + \Lambda_2)u^n + \frac{1}{2}\Delta t(\Lambda_1 + \Lambda_2)^2 u^n$$

$$+ \frac{1}{2}\Delta t^2 \Lambda_1\Lambda_2(\Lambda_1 + \Lambda_2)u^n + \frac{\left(\frac{1}{2}\Delta t^2\right)^2}{\Delta t}\Lambda_2\Lambda_2\Lambda_1\Lambda_1 u^n$$

$$+ \Delta t^{-1}\left(B_2 + \frac{1}{2}\Delta t^2\Lambda_2\Lambda_2\right)\left(e_2^n + e_4^n\right) \qquad (x_1, x_2) \in D \qquad \text{(A8)}$$

This scheme thus has both splitting and boundary errors. Computational experience with this scheme reveals a steady-state solution which depends upon Δt^2, even with the spatial inconsistency removed with MUD.

LOD HYBRID SCHEME

Another complete consistent LOD scheme in two dimensions is the hybrid scheme

$$u^* = B_1 u^n + \left(d_2^n + d_4^n\right) \qquad (x_1, x_2) \in \bar{D}_1 \qquad \text{(A9)}$$

$$A_2 u^{n+1} = u^* + \left(g_1^n + g_3^n\right) \qquad (x_1, x_2) \in \bar{D}_2 \qquad \text{(A10)}$$

The whole-step scheme is

$$\frac{u^{n+1} - u^n}{\Delta t} = (\Lambda_1 + \Lambda_2)u^n + \Delta t\,\Lambda_2\,\frac{\left(u^{n+1} - u^n\right)}{\Delta t} \qquad (x_1, x_2) \in D \qquad \text{(A11)}$$

The scheme is thus observed to have no spatial or temporal inconsistency on the interior of the domain. Computational results confirmed this prediction. The scheme cannot be extended to three dimensions as a complete consistent scheme without adding terms and using MUD.

APPENDIX A

3-D LODQ SCHEME

In three dimensions, the LODQ scheme has a split form very similar to the 2-D case. The split steps are

$$\hat{A}_1 u^{(1)} = Q^n \qquad (x_1, x_2, x_3) \in \bar{D}_1 \qquad \text{(A1 2a)}$$

$$\hat{A}_2 u^{(2)} = u^{(1)} \qquad (x_1, x_2, x_3) \in \bar{D}_2 \qquad \text{(A1 2b)}$$

$$\hat{A}_3 u^{n+1} = u^{(2)} \qquad (x_1, x_2, x_3) \in \bar{D}_3 \qquad \text{(A1 2c)}$$

$$Q^{n+1} = Q^n + \Delta t(\Lambda_1 + \Lambda_2 + \Lambda_3) u^{n+1} \qquad (x_1, x_2, x_3) \in D \qquad \text{(A1 2d)}$$

where $\hat{A}_3$ and $\bar{D}_3$ are defined analogously to $\hat{A}_\ell$ and $\bar{D}_\ell$, with $\ell = 1,2$. The whole-step scheme obtained by eliminating $u^{(1)}$, $u^{(2)}$, and Q is, for steady boundary data,

$$\frac{u^{n+1} - u^n}{\Delta t} = (\Lambda_1 + \Lambda_2 + \Lambda_3)\left[\alpha u^{n+1} + (1 - \alpha) u^n\right]$$

$$- \alpha^2 \Delta t^2 (\Lambda_1\Lambda_2 + \Lambda_1\Lambda_3 + \Lambda_2\Lambda_3) \frac{(u^{n+1} - u^n)}{\Delta t}$$

$$+ \alpha^3 \Delta t^3 \Lambda_1\Lambda_2\Lambda_3 \frac{(u^{n+1} - u^n)}{\Delta t} \qquad \text{(A1 3)}$$

APPENDIX B

STABILITY OF LODQ SCHEME

TWO DIMENSIONS

In this section, the Von Neumann damping ratios for the LODQ scheme are presented for the two-dimensional model equations

$$\frac{\partial u}{\partial t} = \frac{\partial^2 u}{\partial x_1^2} + \frac{\partial^2 u}{\partial x_2^2} \tag{B1}$$

$$\frac{\partial u}{\partial t} = - \frac{\partial u}{\partial x_1} - \frac{\partial u}{\partial x_2} \tag{B2}$$

For the two-dimensional parabolic equation (eq. (B1)), the damping ratio is

$$G = \frac{1 + (\alpha - 1)(\beta_1 + \beta_2) + \alpha^2 \beta_1 \beta_2}{1 + \alpha(\beta_1 + \beta_2) + \alpha^2 \beta_1 \beta_2} \tag{B3}$$

For the two-dimensional hyperbolic equation (eq. (B2)), the damping ratio is, for central-space and backward Euler time differences,

$$G = \frac{(1 - \alpha^2 \eta_1 \eta_2) - (\alpha - 1) i (\eta_1 + \eta_2)}{(1 - \alpha^2 \eta_1 \eta_2) - \alpha i (\eta_1 + \eta_2)} \tag{B4}$$

where $i = \sqrt{-1}$ and $\eta_\ell = \Delta t \, h^{-1} \sin \theta_\ell$. It is easily verified that in both these formulas, $|G| \leq 1$ for all Δt provided that $\frac{1}{2} \leq \alpha \leq 1$.

THREE DIMENSIONS

In this section, the Von Neumann damping ratios for the LODQ scheme are presented for the three-dimensional model equations

APPENDIX B

$$\frac{\partial u}{\partial t} = \frac{\partial^2 u}{\partial x_1^2} + \frac{\partial^2 u}{\partial x_2^2} + \frac{\partial^2 u}{\partial x_3^2} \tag{B5}$$

$$\frac{\partial u}{\partial t} = -\frac{\partial u}{\partial x_1} - \frac{\partial u}{\partial x_2} - \frac{\partial u}{\partial x_3} \tag{B6}$$

For the three-dimensional parabolic equation (eq. (B5)), the damping ratio is

$$G = \frac{1 + (\alpha - 1)(\beta_1 + \beta_2 + \beta_3) + \alpha^2(\beta_1\beta_2 + \beta_1\beta_3 + \beta_2\beta_3) + \alpha^3\beta_1\beta_2\beta_3}{1 + \alpha(\beta_1 + \beta_2 + \beta_3) + \alpha^2(\beta_1\beta_2 + \beta_1\beta_3 + \beta_2\beta_3) + \alpha^3\beta_1\beta_2\beta_3} \tag{B7}$$

Again, from this formula, $|G| \leq 1$ for all Δt for $\frac{1}{2} \leq \alpha \leq 1$. The damping ratio for the three-dimensional hyperbolic equation (eq. (B6)) is

$$G = \frac{\left[1 - \alpha^2(\eta_1\eta_2 + \eta_1\eta_3 + \eta_2\eta_3)\right] + i\left[(\alpha - 1)(\eta_1 + \eta_2 + \eta_3) - \alpha^3\eta_1\eta_2\eta_3\right]}{\left[1 - \alpha^2(\eta_1\eta_2 + \eta_1\eta_3 + \eta_2\eta_3)\right] + i\left[\alpha(\eta_1 + \eta_2 + \eta_3) - \alpha^3\eta_1\eta_2\eta_3\right]} \tag{B8}$$

From equation (B8) we see that the scheme is stable provided

$$\left[(\alpha - 1)(\eta_1 + \eta_2 + \eta_3) - \alpha^3\eta_1\eta_2\eta_3\right]^2 \leq \left[\alpha(\eta_1 + \eta_2 + \eta_3) - \alpha^3\eta_1\eta_2\eta_3\right]^2 \tag{B9}$$

This inequality can never be satisfied for $\Delta t > 0$ for any α in the range $0 \leq \alpha \leq 1$. Thus, the scheme is unconditionally unstable for equation (B6).

REFERENCES

1. Yanenko, N. N. (Northrop Corporate Labs., transl.): The Method of Fractional Steps. Springer-Verlag, 1971.

2. Briley, W. R.; and McDonald, H.: Solution of the Three-Dimensional Compressible Navier-Stokes Equations by an Implicit Technique. Proceedings of the Fourth International Conference on Numerical Methods in Fluid Dynamics. Volume 35 of Lecture Notes in Physics, Robert D. Richtmyer, ed., Springer-Verlag, 1975, pp. 105-110.

3. Beam, Richard M.; and Warming, R. F.: An Implicit Factored Scheme for the Compressible Navier-Stokes Equations. AIAA J., vol. 16, no. 4, Apr. 1978, pp. 393-402.

4. MacCormack, R. W.; and Baldwin, B. S.: A Numerical Method for Solving the Navier-Stokes Equations With Application to Shock-Boundary Layer Interactions. AIAA Paper 75-1, Jan. 1975.

5. Abarbanel, Saul; and Gottlieb, David: Optimal Time Splitting for Two and Three Dimensional Navier-Stokes Equations With Mixed Derivatives. NASA CR-159386, 1980.

6. Beam, Richard M.; and Warming, R. F.: An Implicit Factored Scheme for the Compressible Navier-Stokes Equations II: The Numerical ODE Connection. A Collection of Technical Papers - AIAA Computational Fluid Dynamics Conference, July 1979, pp. 1-13. (Available as AIAA Paper 79-1446.)

7. Mitchell, A. R.: Computational Methods in Partial Differential Equations. John Wiley & Sons, c.1969.

8. Briley, W. R.; and McDonald, H.: On the Structure and Use of Linearized Block Implicit Schemes. J. Comput. Phys., vol. 34, no. 1, Jan. 1980, pp. 54-73.

9. Douglas, Jim, Jr.; and Gunn, James E.: A General Formulation of Alternating Direction Methods. Part I. Parabolic and Hyperbolic Problems. Numer. Math., Bd. 6, 1964, pp. 428-453.

TABLE I.- ERRORS IN SOLUTION TO TP1 AND TP2

USING THE DOUGLAS-GUNN METHOD

$[\tau = 1, 10, 1000]$

h	$\|E\|_{max}$	$\|E\|_{min}$	$\|E\|_{max} \frac{1}{2} h^2$
1/4	2.8239880×10^{-2}	1.6879493×10^{-2}	0.9037
1/8	7.2936317×10^{-3}	1.6010933×10^{-3}	.9336
1/16	1.8392306×10^{-3}	1.2112913×10^{-3}	.9417

TABLE II.- CALCULATED AND PREDICTED MAXIMUM RESIDUALS FOR

TP2 USING LODBEC METHOD

$[h = 1/8]$

τ	$\|R\|_{max}$		
	Calculated by LODBEC	Predicted by eq. (51) (analytic)	Predicted by eq. (51) (discrete)
1	2.4358	2.4674	2.4358
10	243.58	246.74	243.58
1000	2435.8	2467.4	2435.8

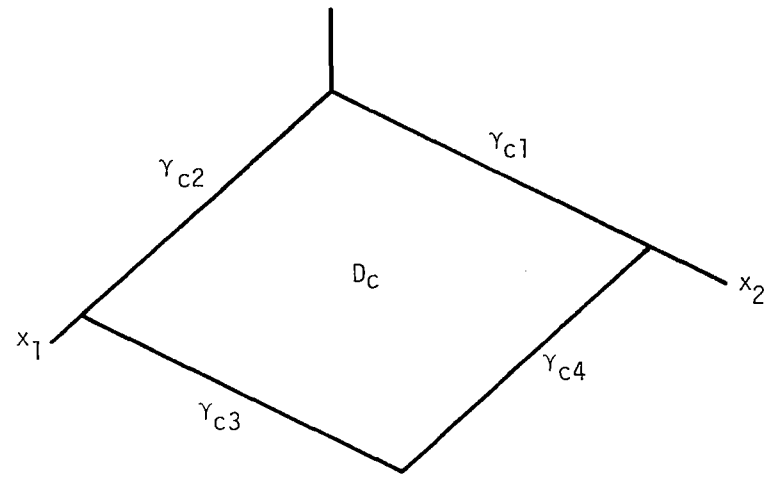

$\Gamma_c = \gamma_{c1} \cup \gamma_{c2} \cup \gamma_{c3} \cup \gamma_{c4}$

Continuum region

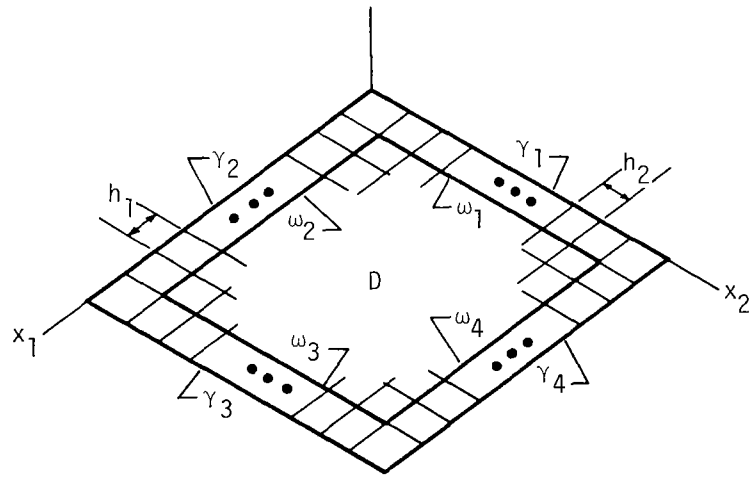

$\Gamma \equiv \gamma_1 \cup \gamma_2 \cup \gamma_3 \cup \gamma_4$

$\Omega \equiv \omega_1 \cup \omega_2 \cup \omega_3 \cup \omega_4$

Discrete region

Figure 1.- Continuum and discrete regions.

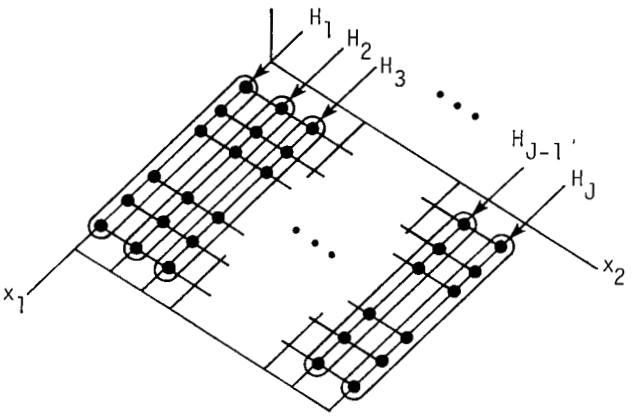

$$D_1 \equiv \bigcup_{j=2}^{J-1} H_j$$

$$\bar{D}_1 \equiv \bigcup_{j=1}^{J} H_j$$

Discrete sets D_1 and $\bar{D}_1$

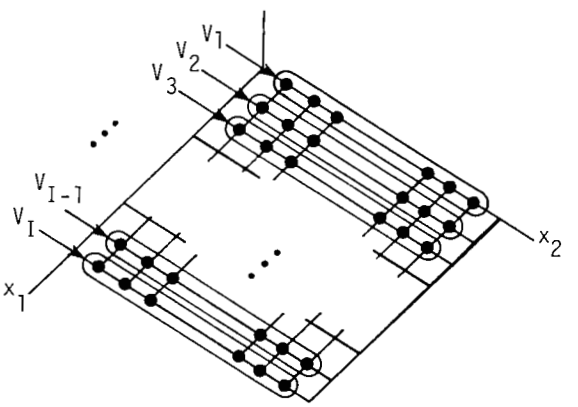

$$D_2 \equiv \bigcup_{i=2}^{I-1} V_i \quad , \quad \bar{D}_2 \equiv \bigcup_{i=1}^{I} V_i$$

Discrete sets D_2 and $\bar{D}_2$

Figure 1.- Concluded.

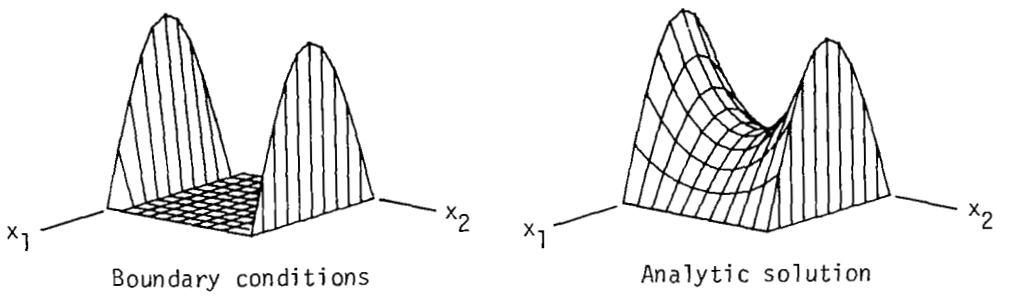

Test problem 1 (TP1)

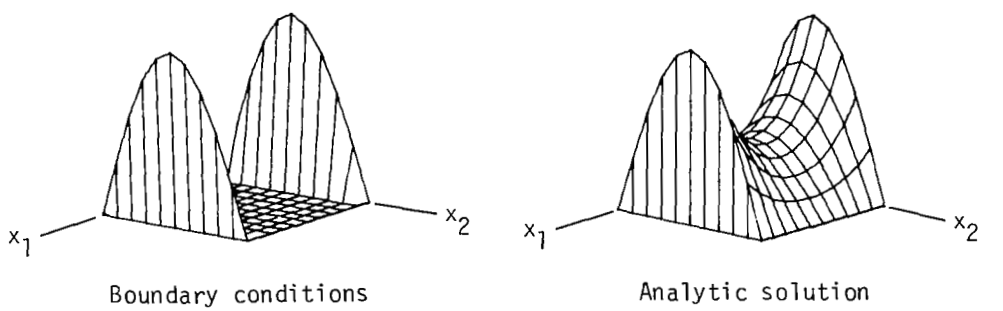

Test problem 2 (TP2)

Figure 2.- Boundary conditions and analytic solutions for the two test problems considered.

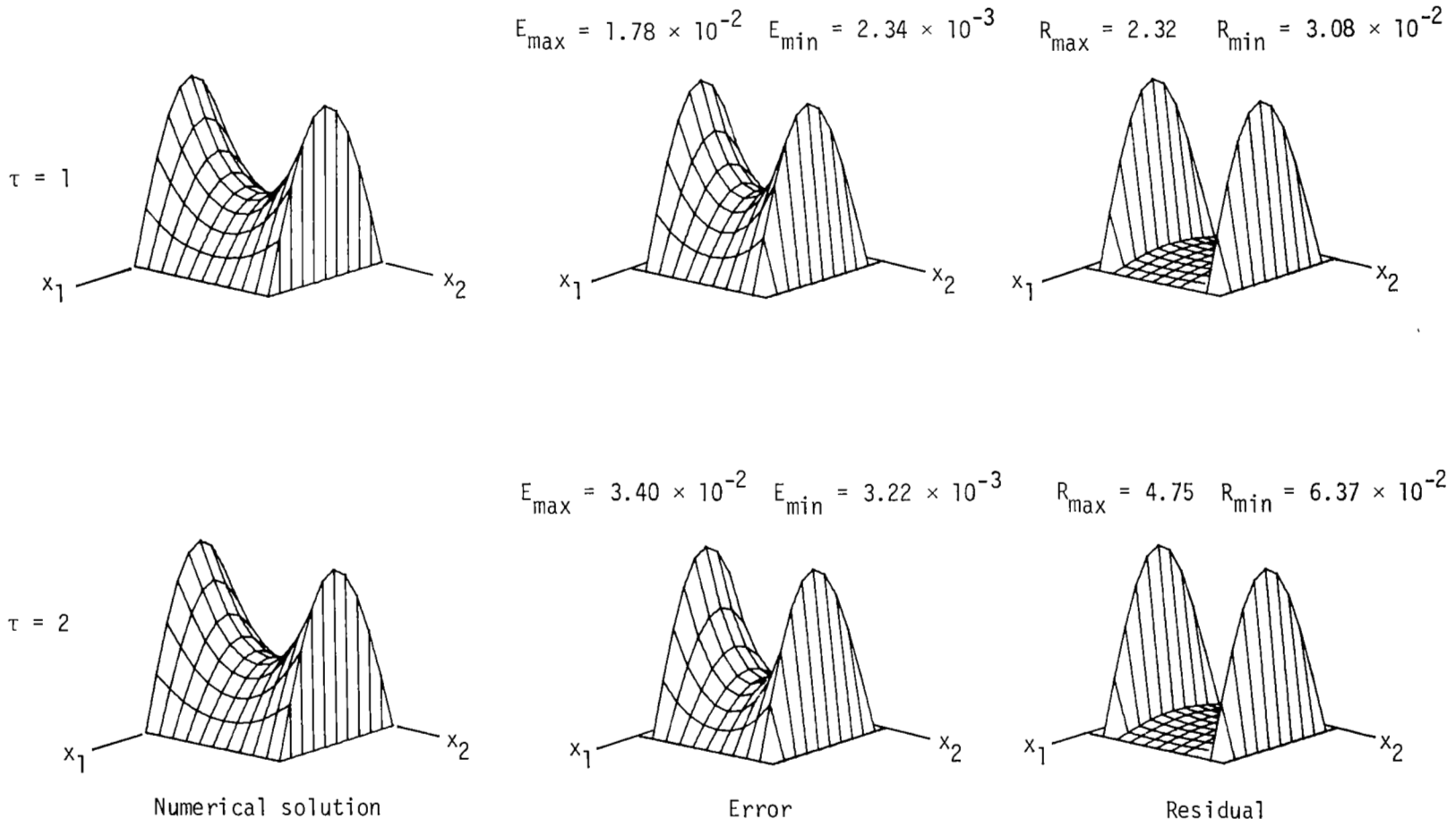

Figure 3.- Numerical results - LOD forward Euler scheme applied to TP1.

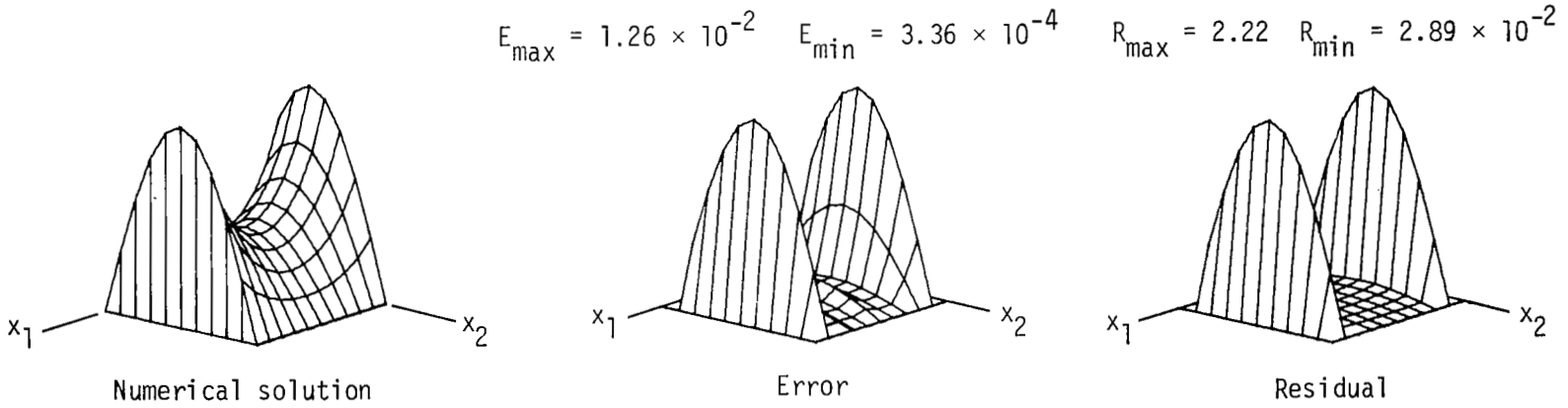

(a) $\tau = 1, \quad h = 0.1.$

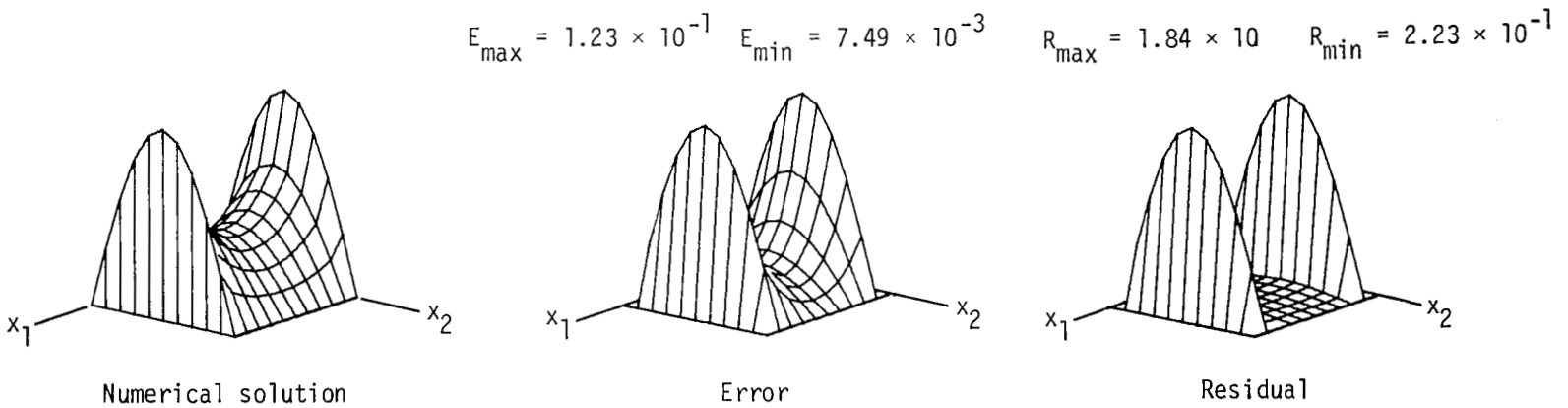

(b) $\tau = 10, \quad h = 0.1.$

Figure 4.- Numerical results - LOD backward Euler scheme applied to TP2.

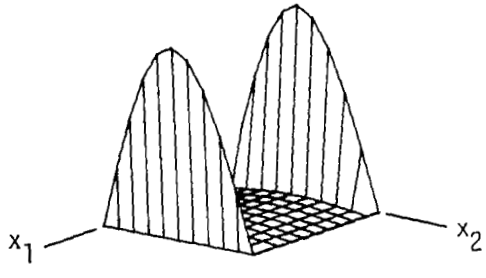

Numerical solution

$E_{max} = 7.18 \times 10^{-1}$ $E_{min} = 1.12 \times 10^{-1}$

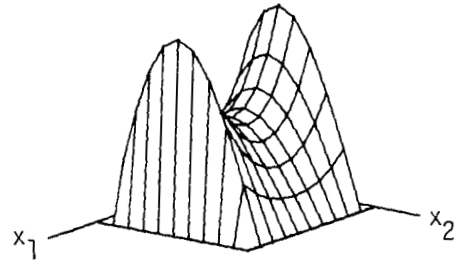

Error

$R_{max} = 9.57 \times 10$ $R_{min} = 1.09 \times 10^{-1}$

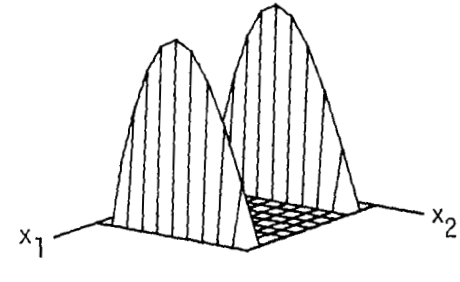

Residual

(c) $\tau = 1000$, $h = 0.1$.

Figure 4.- Concluded.

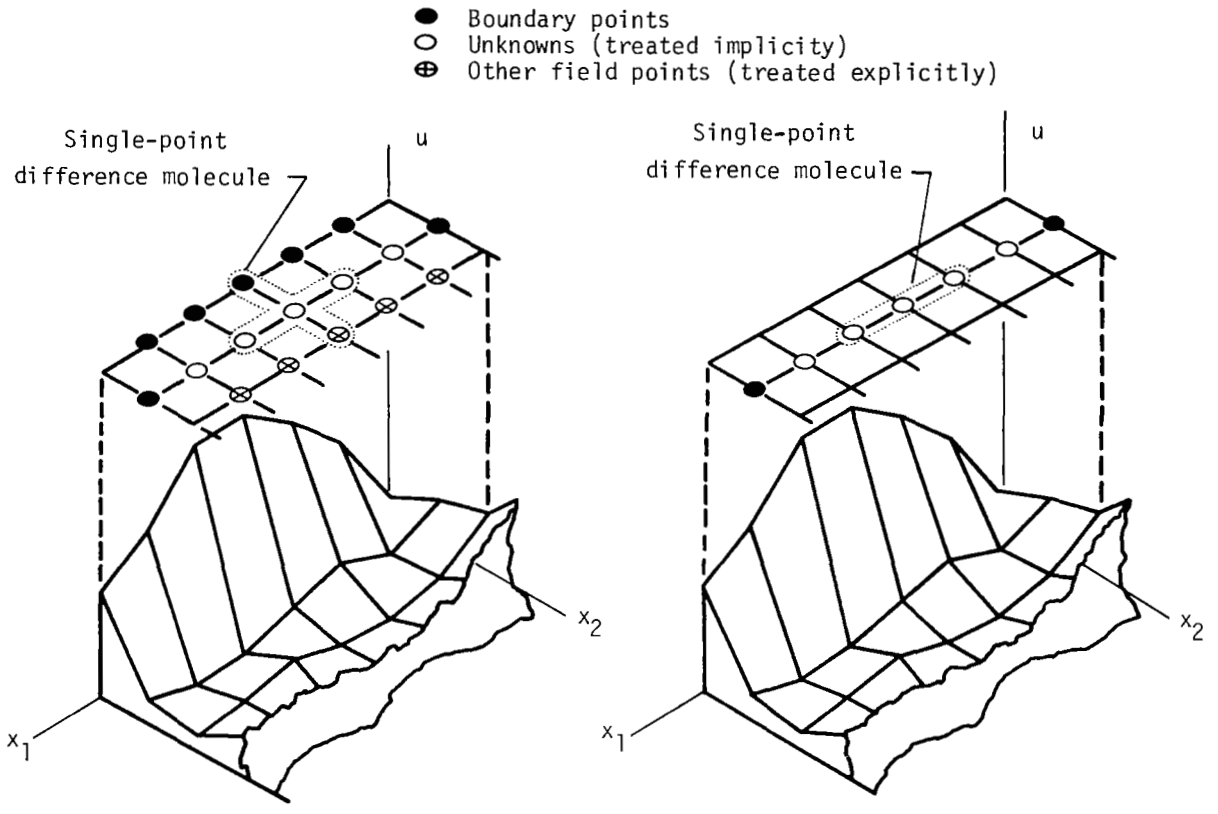

(a) Douglas-Gunn method: x_1 line algorithm.

(b) LOD methods: x_1 line algorithm.

Figure 5.- Comparison of field points used in the line algorithms for the Douglas-Gunn and LOD methods.

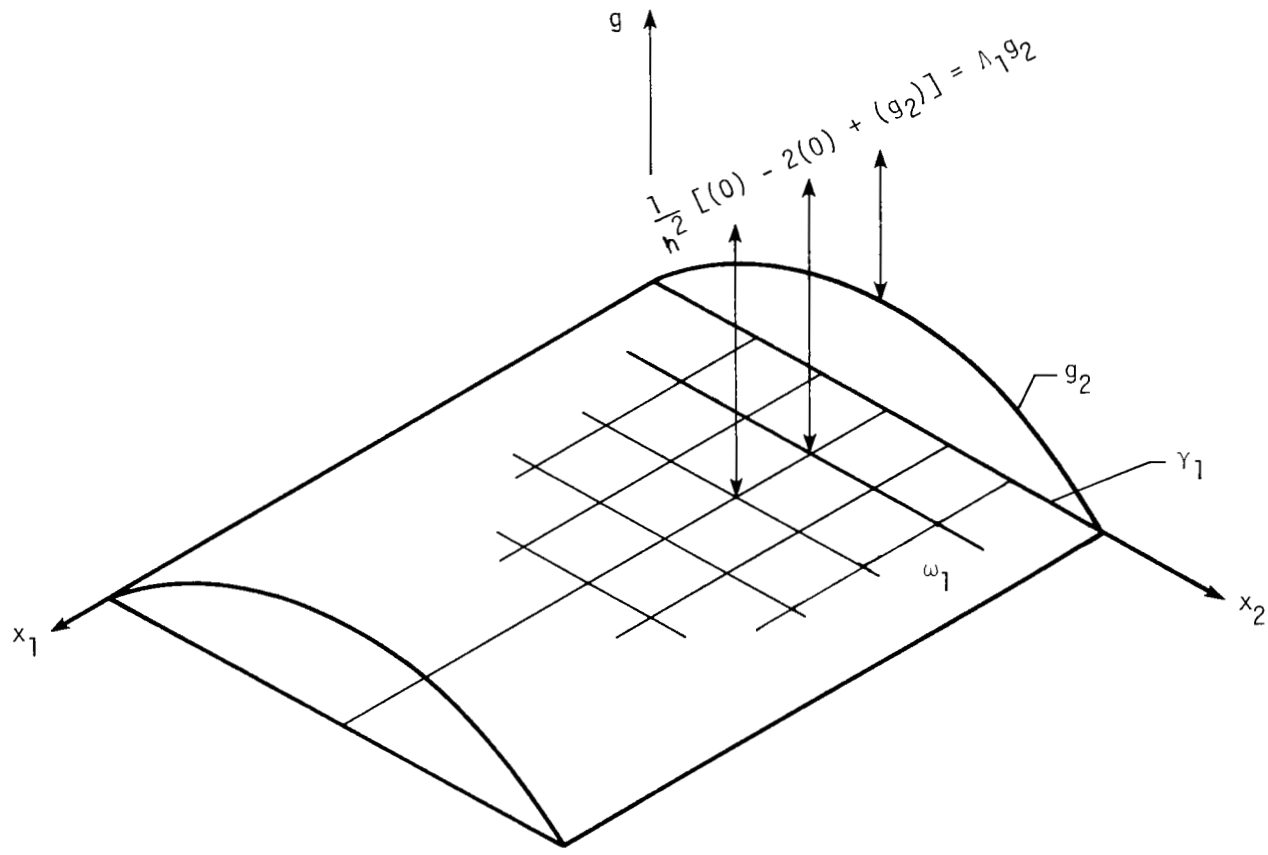

Figure 6.- Propagation of the boundary residual onto the set Ω.

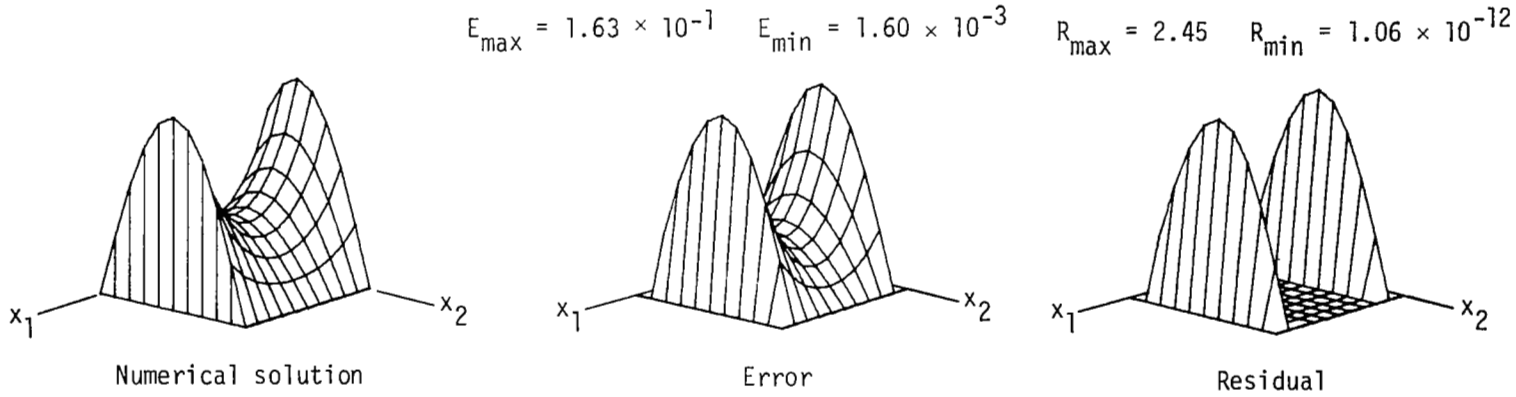

(a) $\tau = 1, \quad h = 0.1.$

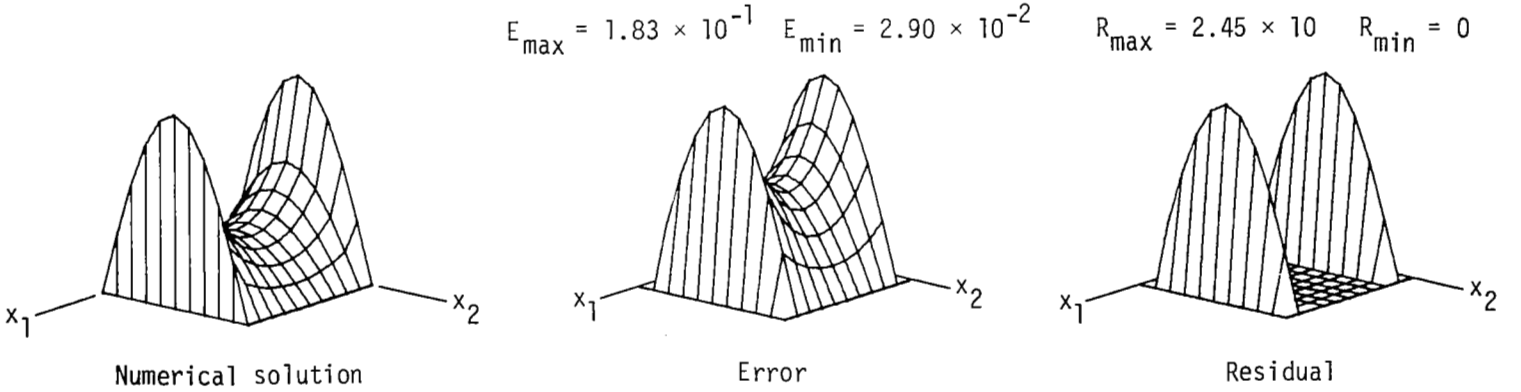

(b) $\tau = 10, \quad h = 0.1.$

Figure 7.- Numerical results - consistent LOD backward Euler scheme applied to TP2.

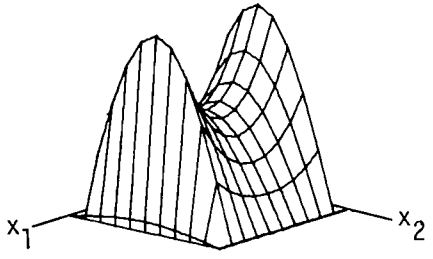

Numerical solution

$E_{max} = 1.86 \times 10$ $E_{min} = 3.05$

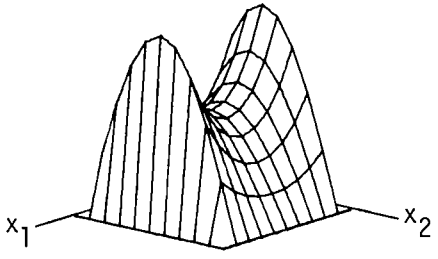

Error

$R_{max} = 2.45 \times 10^{3}$ $R_{min} = 2.47 \times 10^{-12}$

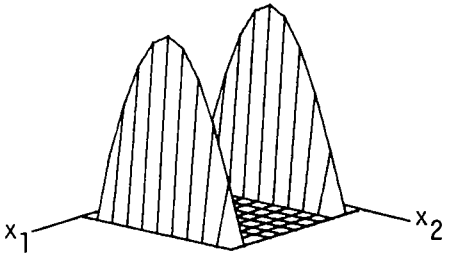

Residual

(c) $\tau = 1000$, $h = 0.1$.

Figure 7.- Concluded.

$E_{max} = 4.63 \times 10^{-3}$ $E_{min} = 1.08 \times 10^{-3}$ $R_{max} = 3.06 \times 10^{-1}$ $R_{min} = 0$

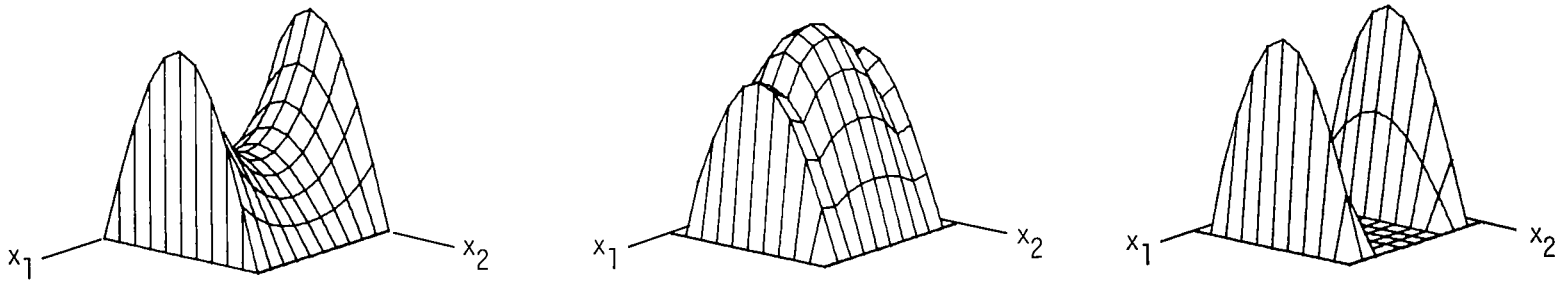

Numerical solution Error Residual

(a) $\tau = 1$, $h = 0.1$.

$E_{max} = 1.44 \times 10^{-1}$ $E_{min} = 4.17 \times 10^{-1}$ $R_{max} = 3.06 \times 10$ $R_{min} = 0$

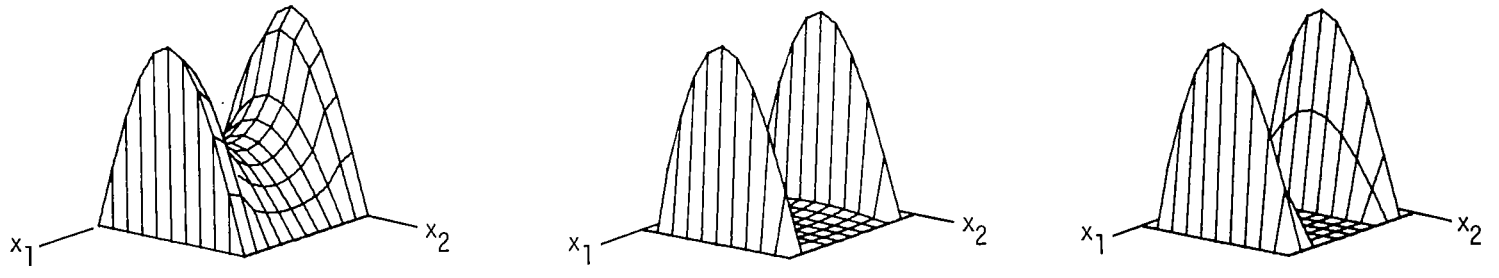

Numerical solution Error Residual

(b) $\tau = 10$, $h = 0.1$.

Figure 8.- Numerical results - LOD predictor-corrector scheme applied to TP2.

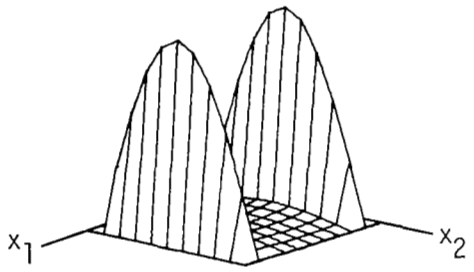

Numerical solution

$E_{max} = 1.42 \times 10^3$ $E_{min} = 1.86 \times 10$

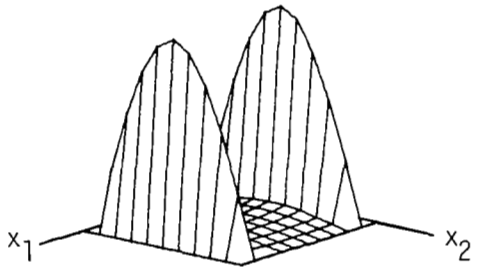

Error

$R_{max} = 3.06 \times 10^5$ $R_{min} = 0$

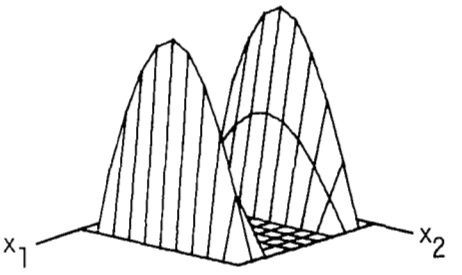

Residual

(c) $\tau = 1000$, $h = 0.1$.

Figure 8.- Concluded.

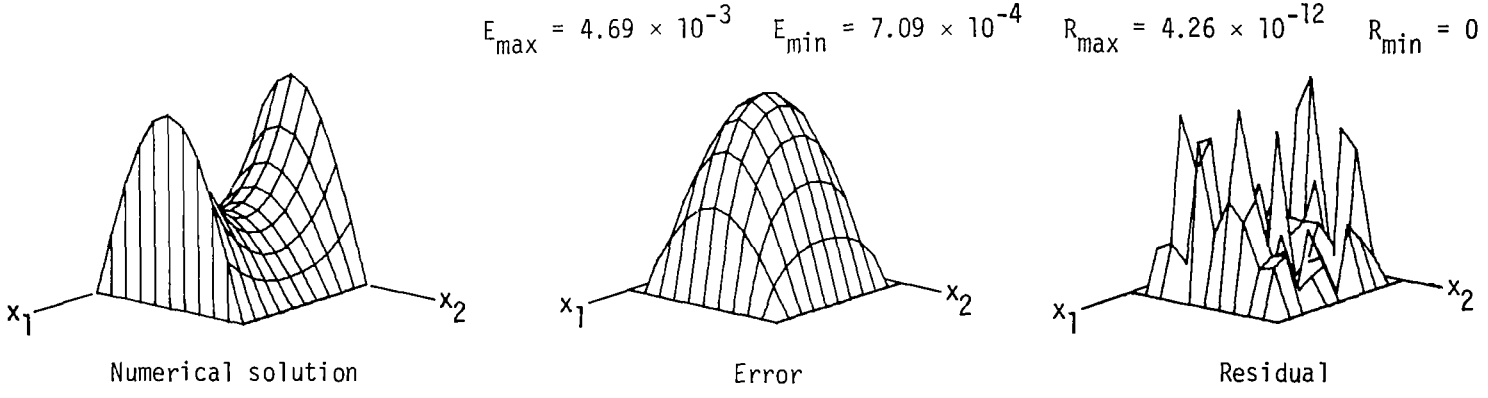

Figure 9.- Numerical results - consistent LOD backward Euler scheme with MUDF applied to TP2. $\tau = 10$; $h = 0.1$.

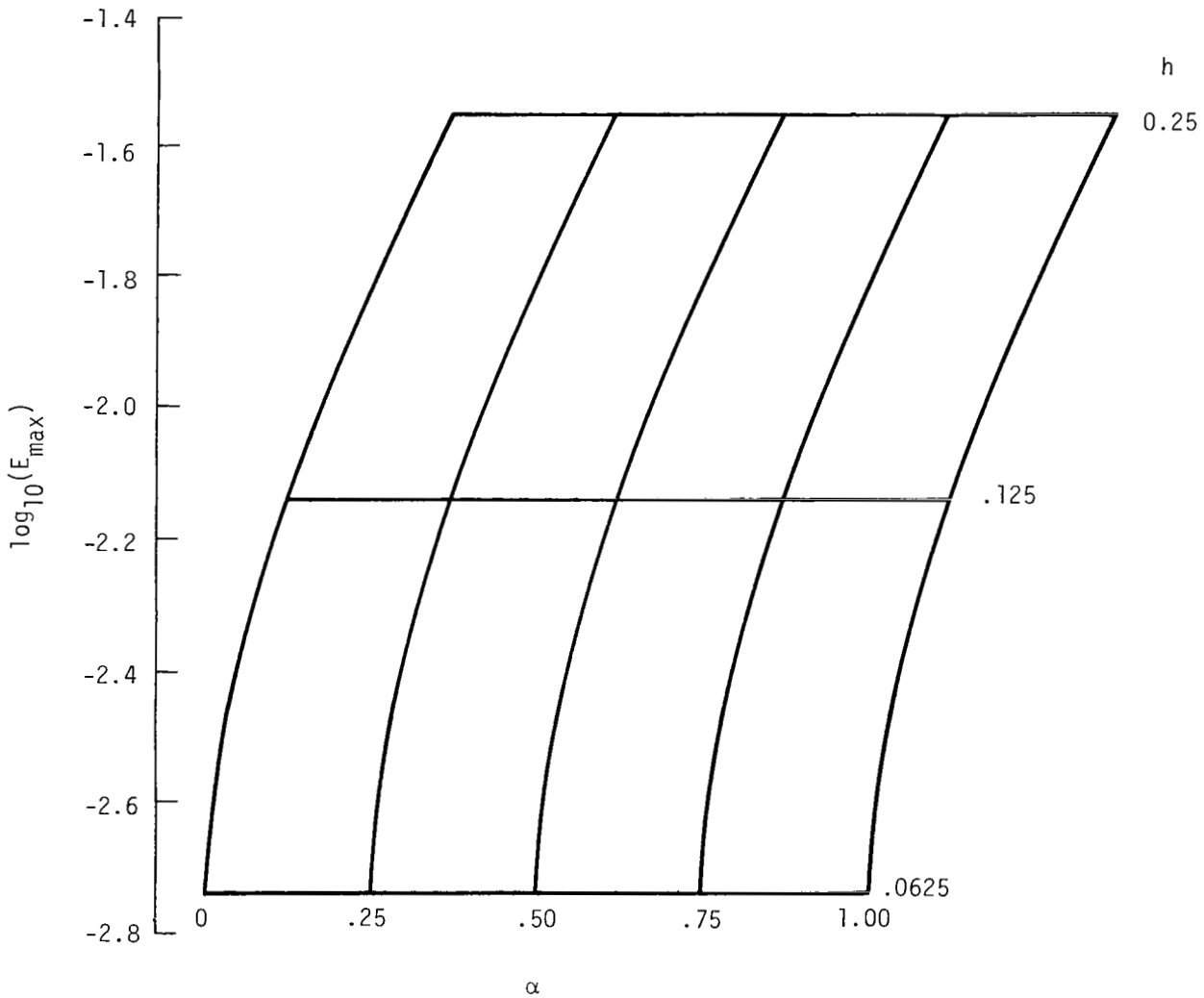

Figure 10.- Solution error of the LODQ scheme applied to TP2.

1. Report No.	2. Government Accession No.	3. Recipient's Catalog No.
NASA TP-1790		

4. Title and Subtitle	5. Report Date
TEMPORAL AND SPATIAL INCONSISTENCIES OF TIME-SPLIT FINITE-DIFFERENCE SCHEMES	April 1981
	6. Performing Organization Code 505-31-33-01
7. Author(s)	8. Performing Organization Report No.
Douglas L. Dwoyer and Frank C. Thames	L-13941
	10. Work Unit No.
9. Performing Organization Name and Address	
NASA Langley Research Center Hampton, VA 23665	11. Contract or Grant No.
	13. Type of Report and Period Covered
12. Sponsoring Agency Name and Address	Technical Paper
National Aeronautics and Space Administration Washington, DC 20546	14. Sponsoring Agency Code

15. Supplementary Notes

16. Abstract

In a recently published work by Abarbanel and Gottlieb (NASA CR-159386), a new class of explicit time-split algorithms designed for application to the Navier-Stokes equations for compressible flow was developed. These algorithms, which utilize locally-one-dimensional (LOD) spatial steps, were shown to possess stability characteristics superior to those of other time-split schemes. In the present work, the properties of an implicit LOD method, analogous to the Abarbanel-Gottlieb algorithm, are examined using the two-dimensional heat conduction equation as the test problem. Both temporal and spatial inconsistencies inherent in the scheme are identified. The principal result of the present work is the development of a new consistent, implicit splitting approach. The relationship between this new method and other time-split implicit schemes is explained, and stability problems encountered with the method in three dimensions are discussed.

17. Key Words (Suggested by Author(s))	18. Distribution Statement
Time-split methods Finite-difference methods	Unclassified - Unlimited Subject Category 64

19. Security Classif. (of this report)	20. Security Classif. (of this page)	21. No. of Pages	22. Price
Unclassified	Unclassified	56	A04

For sale by the National Technical Information Service, Springfield, Virginia 22161

NASA-Langley, 1981